QUARTERLY REPORT

January 1, 2026 – March 31, 2026

Kentucky Tobacco
Research & Development Center

Martin-Gatton
College of Agriculture,
Food and Environment

Martin-Gatton
College of Agriculture,
Food and Environment

MEMORANDUM

DATE: April 30, 2026

TO: Kentucky Tobacco Research Board Members
Legislative Research Commission

FROM: Dr. Ling Yuan
Managing Director, KTRDC

SUBJECT: Kentucky Tobacco Research & Development Center
Quarterly Report for January 1, 2026 – March 31, 2026

Enclosed is a copy of the Kentucky Tobacco Research & Development Center's Quarterly Report for January 1, 2026 – March 31, 2026.

If you have any questions, please feel welcome to contact me at (859) 257-5798 or email lyuan3@uky.edu.

Enc.

TABLE OF CONTENTS

EXECUTIVE SUMMARY

Introduction

The legislation (KRS 248.510 - 248.580) which provides funds in support of the research programs at the Kentucky Tobacco Research and Development Center (KTRDC) requires that a quarterly research report be submitted to the Kentucky Tobacco Research Board (KTRB) and the Legislative Research Commission.

The overall reporting plan is:

January 1	-	March 31:	Selected topics
April 1	-	June 30:	Selected topics
July 1	-	September 30:	Selected topics
October 1	-	December 31:	Annual comprehensive report

As required by KRS 248.570, a financial report covering expenditures for the relevant proportion of the July 1, 2025 – June 30, 2026 fiscal year is included in this report.

The news and research publications provided in this quarterly report are a representative selection of KTRDC's output. For a full description of all KTRDC research and activities please refer to the KTRDC Annual Report.

Quarterly News

- The emphasis in KTRDC's research work continues to be on harm reduction. There is a great deal of collaboration between field and molecular researchers, where the molecular biologists attempt to explain field observations at the cellular level. Examples of these collaborations are:
  - There has been a significant amount of work on tobacco terpenes, such as the CBT diols and cis-abienol. These compounds are of interest because of their effect on tobacco flavor and aroma, and also because they play a role in repelling insects. Molecular scientists are now working on the regulation of terpene formation.
  - A large part of the KTRDC research program, both field and molecular, is devoted to nicotine and nornicotine, particularly lowering these alkaloids in plants.
    - Field and molecular scientists are collaborating to try to understand why the low-alkaloid tobacco lines have such poor leaf quality. It seems that the buildup of nicotine precursors may play a role.

    - The molecular scientists have also identified novel genes that regulate nicotine biosynthesis in plants and are in process to determine the mode of action of these genes.
    - Additionally, molecular scientists have identified novel genes that regulate nicotine to nornicotine conversion in plants and are collaborating in an attempt to determine the mode of action of these genes.
    - Dr. Bob Pearce and Dr. Colin Fisher provided an update on GAP Trainings, which had around 300-400 participants. They received positive feedback from those in attendance and felt they would continue to be beneficial regarding future collaborations and discussions. Dr. Colin Fisher has also attended 15 farmers' meetings where he presented his presentation about the yield decline, which was well received.
- Work at the farm focused mainly on seed cleaning, stripping, grading and seedling production.
    - We were unable to do any stripping in November/December, as we usually do. One trial was stripped and graded in March, and one remains to be stripped: conditions have been unfavorable for bringing the tobacco into case.
    - Seed cleaning and weighing for a seed production trial was done throughout this quarter.
    - Seeding for the 2026 crop was done on March 10 and March 18.
- The March board meeting was held in-person in the McCuiston Conference Room in KTRDC and by Zoom on March 17th 2026.
    - Dr. Colin Fisher of KTRDC gave a presentation entitled "Short-term Improvements to Boost Yield".
        - He outlined decreases in yields over the past several decades, including reasons suggested by growers including the introduction of LC varieties, the potential yield of the new varieties, and the inability to control disease.
        - Grower's average yield for 32 years prior to 1971 increased steadily, most likely due to management style prior to the change in the quota system.
        - Several basic aspects of management that would not require much additional costs were identified, including field site selection, soil

preparation, optimizing seedling size and setting procedures, and using best practices to apply fungicide.

- Dr. Yuan gave an update on the budget.
  - He noted that there has been a reduction in tax income from last year and that it has been trending downward for at least the past several years, but the last few months have been consistent with those in the past.
  - He shared a list of 10 recommendations for future directions of KTRDC which were created by Dr. Yuan, Dr. Matthews, and Mr. Lacefield and included feedback from the board, researchers, and growers. These recommendations have been provided to the Dean's office and are awaiting further comments from the college.

- The calls for papers for the two major conferences have gone out.
  - The CORESTA call for papers was sent out in March, for the Congress (Agronomy-Phytopathology (AP) Conference and Product Science-Product Technology (PSPT) Conference) to be held October 25th – 29th in Victoria Falls, Zimbabwe. Abstracts, due by late May 17th, are being prepared and several KTRDC scientists will attend. The congress theme is "Science for Sustainability and Harm Reduction in the Transforming Tobacco Landscape".
  - The call for papers for the 79th TSRC conference went out in March. The conference will be held September 20th – 23rd in Charlotte, NC. The theme is "The Evolving Landscape of Tobacco Harm Reduction." Abstracts, due in May 15th, are being prepared and several KTRDC scientists will attend.

- The CTRP proficiency testing (PT) program currently covers the certified 1R6F reference cigarette and the certified reference smokeless tobacco products.
  - The current PT rounds are:
    - SMK-2025D – The parameters for this round of testing include Total Nicotine, Free Nicotine, NNK (4-(methylnitrosamino)-1-(3-pyridyl)-1-butanone, NNN (N-nitrosonornicotine), NAT (N-nitrosoanatabine), NAB (N-nitrosoanabasine), pH, Moisture, Acetaldehyde, Crotonaldehyde, Formaldehyde, Benzo[α]pyrene (BaP), Cadmium, and Arsenic using two certified reference smokeless tobacco products: 1S5 (Snus) and 3S1 (Loose Leaf Chewing Tobacco). This round of testing opened in August 2025 and the data portal for participants to upload data closed January 2026. The interim report was released for participant review in January 2026 and the final report was released in March 2026.

- CIG-2026A – The parameters for this round of testing include smoking parameters o-toluidine, 2,6-dimethylanilin, o-anisidine, 1-aminonaphthalene, 2-aminonaphthalene, 3-aminobiphenyl, 4-aminobiphenyl, Total Particulate Matter (TPM), Puff Count, Benzo[α]pyrene (BaP), BaP-Total Particulate Matter (BaP-TPM) and BaP-Puff Count Parameters using the 1R6F reference cigarette as proficiency test material smoked in both Non-Intense and the Intense smoking regimes. This round of testing opened in January 2026 and the data portal for participants to upload data will close in April 2026. The interim report is scheduled to be released for participant review in May 2026 and the final report is scheduled to be released May 2026.
- CIG-2026B – The parameters for this round of testing include smoking parameters Ammonia, Acrylonitrile, Isoprene, Benzene, Toluene, 1,3 – Butadiene, Total Particulate Matter, and Puff Count Parameters using the 1R6F reference cigarette as proficiency test material smoked in both Non-Intense and the Intense smoking regimes. This round of testing opened in March 2026 and the data portal for participants to upload data is scheduled to close in June 2026.

I would like to thank Mr. Matthew Craft, Ms. Anne Fisher, and Sitakanta Pattanaik for their help with writing some sections of this report, and Mr. Matthew Craft and Ms. Cortney Berry for their help with the compilation.

The KTRDC Quarterly Reports include a copy and brief summary of work published by KTRDC scientists and scientists partly supported by KTRDC.

Report #1 "Post-translational control of biotic stress-related nicotine biosynthesis by a MAP kinase signaling cascade".

Yan Zhou, Yongliang Liu, Ruiqing Lyu, Sanjay Kumar Singh, Xueyi Sui, Xin Hou, Sitakanta Pattanaik, Ling Yuan

This research relates to extracellular signals capable of triggering a variety of cellular responses. The characterization of the MAPK cascade that promotes nicotine biosynthesis is described. RNAi-mediated silencing and induced-overexpression of a portion of the cascade have been shown to impact the nicotine content in tobacco hairy roots. This work highlights the importance of posttranslational regulation of nicotine biosynthesis.

The evolutionarily conserved mitogen-activated protein kinase (MAPK) cascades relay extracellular signals into cells, triggering a variety of cellular responses. We previously revealed NtMPK4 as a positive regulator of nicotine biosynthesis; however, its upstream regulation remains unclear. Here, we characterized a MAPK cascade, comprising NtMEKK1b, NtMPKK2a, and NtMPK4, that promotes nicotine biosynthesis. This signaling module transduces external cues, including jasmonate and pathogen elicitors such as flg22, into post-translational modifications that enhance transcriptional activity and pathway gene expression. NtMPKK2a physically interacts with and phosphorylates NtMPK4 in vivo, confirming its role as an upstream kinase. RNAi-mediated silencing of NtMPKK2a significantly reduced the expression of nicotine pathway genes and decreased nicotine accumulation, whereas induced-overexpression of NtMPKK2a upregulated nicotine pathway genes and increased nicotine contents in tobacco hairy roots. Overexpression of NtMPKK2a in tobacco cells enhanced the transactivation activity of a NIC2-locus Ethylene Response Factor NtERF221 on Putrescine N-methyltransferase (NtPMT) promotor, further supporting its role in promoting nicotine biosynthesis. Furthermore, we identified NtMEKK1b, a tobacco MEKK that interacts with NtMAPKK2a in yeast cells. Knock-down of NtMEKK1b in transgenic tobacco plants attenuated the expression of nicotine pathway genes and reduced nicotine contents, whereas induced overexpression of NtMEKK1b upregulated gene expression and nicotine accumulation. Our findings uncover a previously uncharacterized MAPK cascade module, NtMEKK1b-NtMPKK2a-NtMPK4, that regulates nicotine biosynthesis, highlighting the importance of posttranslational regulation in nicotine biosynthesis.

Report #2 "Comparison of the 1C2 Reference Filtered Cigar to the 1R6F Reference Filtered Cigarette"

Amrita Machwe, Samuel B. Clark, Halle Harned, Tanvi Sawardekar, Stacey A. Slone, Huihua Ji, David K. Orren

This research compares the toxicity of the smoke condensate from the reference filtered cigar (1C2) and the certified reference cigarette (1R6F) manufactured as part of a collaborative agreement with the FDA. The smoke condensate was generated using the three primary smoking regimes for combustible tobacco products. The condensates from 1C2 resulted in higher toxicity than condensate from the 1R6F when prepared under the same conditions. This suggests that some filtered cigars may be at least as harmful to consumers as conventional cigarettes.

Filtered cigars are a class of tobacco products that can be consumed similarly as conventional cigarettes. Here we have compared tobacco smoke condensates prepared from the 1C2 reference filtered cigar with those from the 1R6F reference cigarette with respect to effects on cell proliferation and viability and AhR-mediated gene expression. Tobacco smoke condensates were prepared using ISO, Health Canada Intense (HCI) or Cigar Smoking (CSR) regimens and certain HPHCs were measured. Cell proliferation and viability assays were performed on immortalized human bronchial or oral epithelial cell lines. AHR-mediated gene expression was measured using a mouse hepatoma cell line engineered to express luciferase under control of the AHR promoter. Comparison of different smoking regimens found that the HCI regimen produces higher TPM levels, and higher AhR-mediated gene expression and toxicity when normalized to filler weight. Condensates from 1C2 reference filtered cigars resulted in higher AhR-mediated gene expression and reduced cell viability when compared with condensates prepared under the same conditions from the 1R6F reference cigarettes, again when normalized to filler weight. Our results indicate that this reference filtered cigar is somewhat more toxic than the reference cigarette with the HCI regimen being most toxic. Our findings also suggest that some commercial filtered cigars may have at least as strong toxic effects as conventional cigarettes. This study indicates that, if compared by filler weight, the 1C2 reference filtered cigar is more toxic than the 1R6F reference cigarette. Since these products were manufactured based on commercial products and at least some consumers of filtered cigars inhale smoke from these products into the lung, this suggests that some filtered cigars will be at least as harmful to consumers as conventional cigarettes.

The Crop Journal 14 (2026) 201–213

Contents lists available at ScienceDirect

The Crop Journal

journal homepage: www.keaipublishing.com/en/journals/the-crop-journal/

Post-translational control of biotic stress-related nicotine biosynthesis by a MAP kinase signaling cascade

Yan Zhou [a], Yongliang Liu [a], Ruiqing Lyu [a], Sanjay Kumar Singh [a], Xueyi Sui [b], Xin Hou [c], Sitakanta Pattanaik [a,*], Ling Yuan [a,*]

[a] Department of Plant and Soil Sciences, Kentucky Tobacco Research and Development Center, University of Kentucky, Lexington, KY 40546, USA
[b] Tobacco Breeding and Biotechnology Research Center, Yunnan Academy of Tobacco Agricultural Sciences, Kunming 650201, Yunnan, China
[c] Department of Tobacco, College of Plant Protection, Shandong Agricultural University, Shandong Province Key Laboratory of Agricultural Microbiology, Tai'an 271018, Shandong, China

ARTICLE INFO

Article history:
Received 9 June 2025
Revised 12 August 2025
Accepted 10 September 2025
Available online 25 September 2025

Keywords:
Nicotine biosynthesis
Specialized metabolites
MAPK cascade
Post-translational regulation
Alkaloid biosynthesis
Structural modeling

ABSTRACT

The evolutionarily conserved mitogen-activated protein kinase (MAPK) cascades relay extracellular signals into cells, triggering a variety of cellular responses. We previously revealed NtMPK4 as a positive regulator of nicotine biosynthesis; however, its upstream regulation remains unclear. Here, we characterized a MAPK cascade, comprising NtMEKK1b, NtMPKK2a, and NtMPK4, that promotes nicotine biosynthesis. This signaling module transduces external cues, including jasmonate and pathogen elicitors such as flg22, into post-translational modifications that enhance transcriptional activity and pathway gene expression. NtMPKK2a physically interacts with and phosphorylates NtMPK4 *in vivo*, confirming its role as an upstream kinase. RNAi-mediated silencing of *NtMPKK2a* significantly reduced the expression of nicotine pathway genes and decreased nicotine accumulation, whereas induced-overexpression of *NtMPKK2a* upregulated nicotine pathway genes and increased nicotine contents in tobacco hairy roots. Overexpression of *NtMPKK2a* in tobacco cells enhanced the transactivation activity of a *NIC2*-locus *Ethylene Response Factor NtERF221* on *Putrescine N-methyltransferase* (*NtPMT*) promotor, further supporting its role in promoting nicotine biosynthesis. Furthermore, we identified NtMEKK1b, a tobacco MEKK that interacts with NtMAPKK2a in yeast cells. Knock-down of *NtMEKK1b* in transgenic tobacco plants attenuated the expression of nicotine pathway genes and reduced nicotine contents, whereas induced-overexpression of *NtMEKK1b* upregulated gene expression and nicotine accumulation. Our findings uncover a previously uncharacterized MAPK cascade module, NtMEKK1b-NtMPKK2a-NtMPK4, that regulates nicotine biosynthesis, highlighting the importance of posttranslational regulation in nicotine biosynthesis.

1. Introduction

Tobacco (*Nicotiana tabacum*) is one of the most commercially cultivated crops. Nicotine is a well-studied addictive and harmful compound in tobacco [1], accounting for 90% of the total alkaloids produced in the plant [2]. Biotic stresses, such as insect and microbial attacks, induce the phytohormone jasmonic acid (JA), which in turn promotes nicotine biosynthesis [3,4]. Structurally, nicotine consists of a pyridine ring and a pyrrolidine ring, and its biosynthesis proceeds through three main steps: pyridine ring synthesis, pyrrolidine ring synthesis, and ring conjugation (Fig. 1A). The pyridine ring is derived from aspartate via the NAD biosynthetic pathway, whereas the pyrrolidine ring synthesis originates from the polyamine pathway [5]. Key enzymes involved in nicotine biosynthesis have been identified and functionally characterized, including PMT (putrescine methyltransferase), QPT (quinolinate phosphoribosyltransferase), BBL (berberine bridge-like protein), and A622 [2,6,7]. Nicotine biosynthesis is induced by JA and is regulated by several JA-responsive transcription factors (TFs), including the basic helix-loop-helix (bHLH) TF MYC2 and Apetala2/Ethylene Responsive Factors (AP2/ERFs) such as ERF189, ERF199 and ERF221 [6,7]. Additional TF families, including bZIP, NAC, and WRKY, have also been implicated in the regulation of nicotine biosynthesis [2,6].

* Corresponding authors.
E-mail addresses: spatt2@uky.edu (S. Pattanaik), lyuan3@uky.edu (L. Yuan).

https://doi.org/10.1016/j.cj.2025.08.012

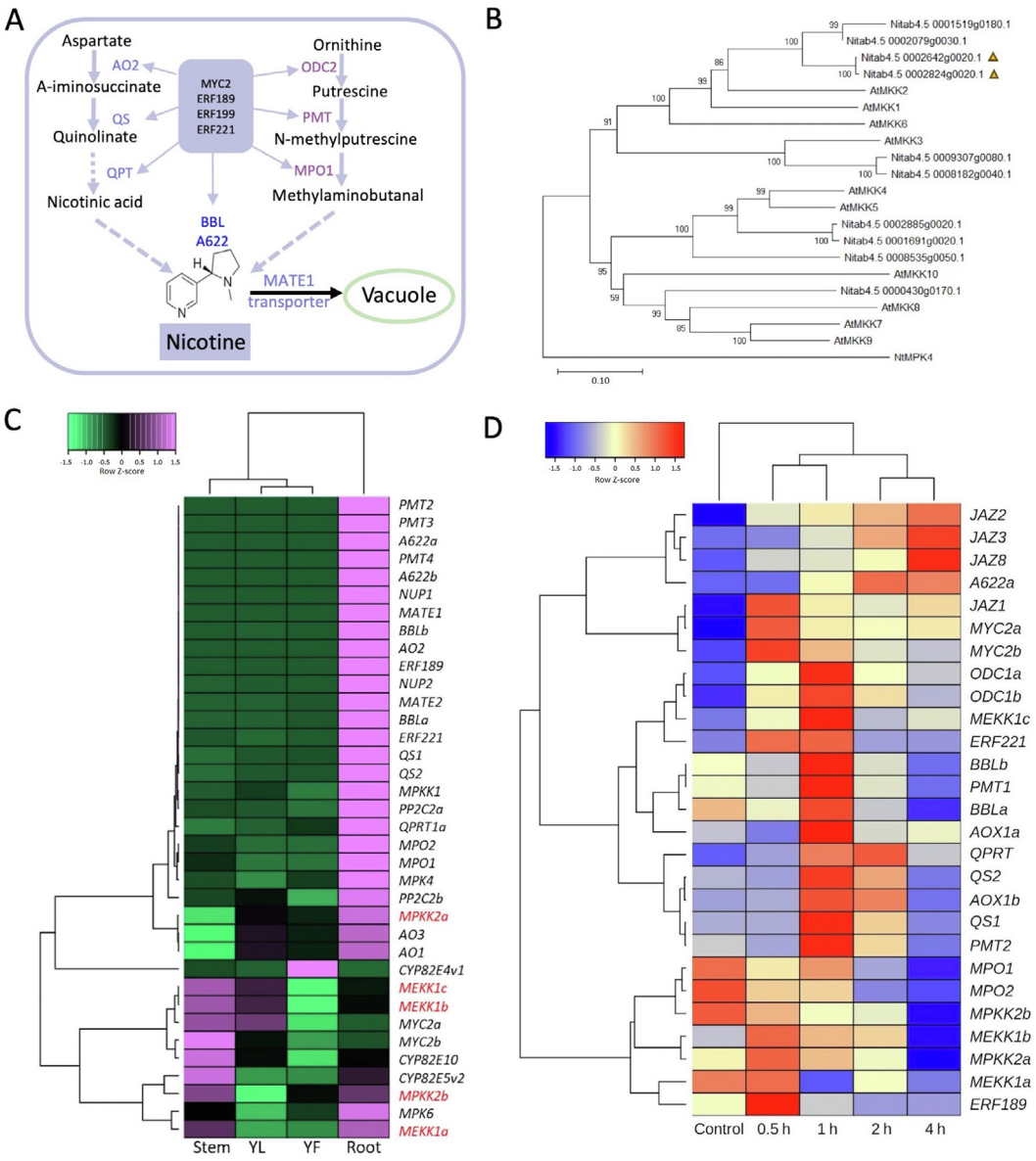

Fig. 1. Identification and expression analysis of *NtMEKK1s* and *NtMAPKK2s*. (A) A schematic diagram of nicotine biosynthesis and regulation in tobacco. (B) Phylogenetic analysis of *AtMAPKKs* and *NtMAPKKs*. The two *NtMPKK2s* candidates characterized in this study are indicated by triangles. (C) A heat-map shows expression profiles of nicotine pathway genes and *NtMPKK2s* and *NtMEKK1s* in stem, young leaf (YL), young flower (YF), and root. (D) A heat-map shows expression profiles of nicotine pathway genes and *NtMPKK2s* and *NtMEKK1s* in JA-treated tobacco roots. Co-expression analysis was performed using transcriptomes of tobacco roots treated with JA for 0.5 h, 1 h, and 4 h. *AO2*, *aspartate oxidase 2*; *ODC2*, *ornithine decarboxylase 2*; *MPO*, *N-methylputrescine oxidase*; *QPT*, *quinolinate phosphoribosyltransferase*; *QS*, *quinolinate synthase*; *PMT*, *putrescine N-methyltransferase*; *A622*, *isoflavone reductase-like protein*; *BBL*, *berberine bridge enzyme-like*; *MATE1*, *Multidrug and Toxic Compound Extrusion transporter*; *ERF*, *Ethylene Response Factor*.

Major attempts to suppress nicotine production in tobacco by silencing known TFs or enzymes involved in the nicotine pathway, such as the ERFs, A622, or BBL, have achieved limited successes, with residual nicotine levels still detectable or sever growth defect [8,9]. This suggests the involvement of additional regulatory mechanisms beyond transcriptional control. In contrast to transcriptional regulation, posttranslational regulation of nicotine biosynthesis remains relatively underexplored. A previous study has demonstrated that the application of a mitogen-activated protein kinase (MAPK) inhibitor, PD98059, reduced the JA-induced transactivation by ERF221 on the *PMT2* and *QPT2* promoters, implicating MAPK signaling in JA-mediated nicotine biosynthesis. Furthermore, transient co-expression of *JA-factor stimulating MAPKK1* (*JAM1*) with *bHLH1* and *ERF221* significantly enhances the transactivation activity of *PMT2* and *QPT2* promoters in tobacco cells [10]. However, the effect of JAM1 on nicotine accumulation and the identity of the downstream MAPK components remain unknown.

Phosphorylation-dephosphorylation is an ancient and evolutionarily conserved mechanism that regulates nearly all biological processes in plants and animals. Protein kinases (PKs), which mediate phosphorylation, represent one of the largest enzyme families in eukaryotes [11]. The genomes of Arabidopsis and rice encode approximately 1000 and 1500 protein kinase, respectively, numbers significantly higher than those found in human (~518) and yeast (~130) [11,12]. Protein phosphorylation plays critical regulatory roles in plant growth and development, phytohormone

biosynthesis and signaling, and responses to biotic and abiotic stresses. Despite the rapid advances in whole-genome sequencing and transcriptomic analyses, which have expanded the catalog of plant protein kinases, functional characterization remains limited for the majority of them. Among the various PK families, MAPKs are the most extensively studied in plants [13]. A canonical MAPK cascade consists of three sequentially acting components: a MAP kinase kinase kinase (MAPKKK/MEKK), a MAP kinase kinase (MAPKK/MEK), and a MAPK. Upon perception of external stimuli, MAPKKKs are activated and phosphorylate MAPKKs, which subsequently phosphorylate and activate MAPKs. Activated MAPKs then phosphorylate a wide range of downstream substrates, including transcription factors and metabolic enzymes, thereby altering their activity, stability, or subcellular localization [14]. These phosphorylation events ultimately modulate developmental and metabolic processes. MAPKs have been implicated in diverse biological functions, including phytohormone signaling, disease resistance, abiotic stress such as cold, salt, and submergence tolerance, light signaling and development [14]. While a number of PKs have been identified as regulators of plant specialized metabolism, their number remains relatively low compared to those involved in other biological processes in plants [15,16].

We have previously demonstrated that overexpression of the tobacco *NtMPK4* increases the expression of nicotine pathway genes and enhances nicotine accumulation in tobacco hairy roots, suggesting that NtMPK4 positively regulates nicotine biosynthesis. However, the upstream components, MAPKKK and MAPKK acting upstream of NtMPK4, and their roles in regulating nicotine biosynthesis remains unknown. Here, we report the identification of a MAP kinase cascade module, NtMEKK1b-NtMPKK2a-NtMPK4, that regulates nicotine biosynthesis in tobacco. Protein-protein interactions among these kinases were validated using yeast two-hybrid and Luciferase Complementation Imaging (LCI) assays, and AlphaFold structural modeling. Phos-tag assay confirmed that the NtMPKK2a phosphorylates NtMPK4 in planta. In addition, transactivation assays demonstrated that both NtMEKK1b and NtMPKK2a enhance the transactivation activity of NtERF221 on the *PMT* promoter. Overexpression or RNAi-mediated silencing of *NtMAPKK2a* or *NtMEKK1b* in tobacco hairy roots altered the nicotine pathway gene expression and affected nicotine accumulation. We also showed that JA and bacterial elicitor, flg22, trigger the activation of the MAP kinase cascade. Together, these findings establish a positive regulatory role for NtMPKK2a, while suggesting a more complex or context-dependent role for NtMEKK1b in controlling nicotine biosynthesis in tobacco. Our work reveals a previously uncharacterized regulatory mechanism by which nicotine biosynthesis is modulated in response to environmental biotic cues. This study highlights the significance of post-translational regulation in specialized metabolism and provides potential targets for the development of low-nicotine tobacco varieties.

2. Materials and methods

2.1. Plant materials and treatments

Nicotiana tabacum '*Samsun NN*' was used for gene cloning, generation of hairy roots and transgenic plants. *Nicotiana benthamiana* was used in all *Agro*-infiltration experiments. For JA treatments, one-month-old tobacco seedlings were treated with 100 μmol L^{-1} methyljasmonate (MeJA; Sigma-Aldrich, St. Louis, MO, USA). For flagellin 22 (flg22) treatments, 1 μmol L^{-1} flg22 were sprayed on tobacco seedlings. For DEX (dexamethasone, Sigma-Aldrich USA) induction of pTA7001-*NtMPKK2a* and *pTA-NtMEKK1b* overexpression lines, DEX (30 μmol L^{-1}) was added to Murashige and Skoog (MS) medium, and the hairy roots were incubated for 16 h before being used for RNA isolation and alkaloid measurement [17]. To measure gene expression and nicotine contents, *pCAMBIA2301-NtMPKK2a-RNAi* and *EV* hairy root lines were inoculated in liquid medium and roots were collected after 4 weeks. For *pCAMBIA2301-NtMEKK1b-RNAi* transgenic plants, *EV* and *RNAi* lines were germinated on half-strength MS medium with 100 mg L^{-1} kanamycin. The top two fully expanded leaves were collected from plants and were used for measurement of nicotine content.

2.2. Generation of transgenic tobacco hairy roots and plants

For RNAi plasmid construction, a 200-bp fragment of *NtMPKK2a* and a 210-bp fragment from *NtMEKK1b* (Table S1) were PCR-amplified and individually ligated into the pKYLX80 vector in both sense and antisense orientations, flanking the *Glycine max FAD3* intron [18]. The resulting sense and antisense fragments with the *FAD3* intron were excised from pKYLX80 and ligated to a modified pCAMBIA2301 vector containing the *CaMV*35S promoter and *rbcS* terminator. The pCAMBIA2301 empty vector was used as control. For conditional overexpression, *NtMPKK2a* and *NtMEKK1b* were individually cloned in pTA7001 vector under the control of a DEX-inducible promoter [19]. For generation of hairy roots, the plasmids were mobilized into *Agrobacterium rhizogenes* K599 by freeze–thaw. Transformation of tobacco leaf discs and generation of hairy roots were performed using the protocol described previously [20]. Transgenic status of the hairy root lines was verified by PCR amplification of marker genes. For generation of stable transgenic tobacco plants, the plasmids were mobilized into *Agrobacterium tumefaciens* GV3850. Tobacco leaf disc transformation and generation of transgenic plants was performed as previously described [21]. Two independent hairy roots or transgenic tobacco lines were selected for further analysis.

2.3. Sequence alignments and phylogenetic analysis

To identify the *NtMPKK2* and *NtMEKK1* genes in *N. tabacum,* amino acid sequences of all Arabidopsis *MPKKs* and *MEKKs* family genes were retrieved from the TAIR database (https://www.arabidopsis.org). These sequences were then used as queries to perform Basic Local Alignment Search Tool (BLAST) searches with default settings against the *N. tabacum* reference sequences downloaded from the *Sol Genomics Network database* [22]. Subsequently, the full-length protein sequences of *MAPKK* and *MEKK* genes from both tobacco and Arabidopsis were aligned using ClustalW with default settings. MEGA6.0 was used to construct the phylogenetic tree using the neighbor-joining (NJ) method with bootstrap values set as 1000 replicates.

2.4. Transcriptome analysis

To determine the spatiotemporal expression of *NtMPKK2s*, *NtMEKK1s* and nicotine pathway-related genes in *N. tabacum*, RNA-seq data of different tissues (stem, leaf, root, and flower) were obtained from the sequence read archive database (SRA, accession number PRJNA208209). RNA-seq data of tobacco roots treated with JA was generated in-house [23]. Raw Illumina sequence reads were processed using the prinseqlite-0.20.4 to remove low-quality reads [24]. Subsequently, pre-processed reads were assessed for quality control using FastQC (version 0.11.3; Babraham Bioinformatics, Cambridge, UK). Read mapping was performed by Bowtie2 [25] using the reference sequence downloaded from the *Sol Genomics Network database* [26]. The $\log_2$ fragments per kilobase of transcript per million mapped reads (FPKM) was used for clustering calculation and visualization by 'stats' and 'ggplot2' packages in R (https://www.R-project.org/; https://CRAN.R-project.org/package=gplots).

2.5. Yeast two-hybrid assay

The full-length cDNA of *NtMPKK2a or NtMPKK2b* was cloned into *pAD-GAL4*, and *NtMPK4*, *NtMEKK1a*, *NtMEKK1b*, or *NtMEKK1c* was cloned into *pBD-GAL4-Cam* (Stratagene, La Jolla, CA, USA). The combination of different AD or BD plasmids were co-transformed into yeast strain *AH109* using the PEG/LiCl method (Clontech, Mountain View, CA, USA), and transformed cells were selected on Synthetic Dropout (SD) medium lacking leucine and tryptophan (–LT). Individual colonies from the plates were chosen and then streaked on SD medium lacking histidine, leucine, tryptophan (–HLT) or lacking adenine, histidine, leucine, tryptophan (–AHLT) to verify protein–protein interactions.

2.6. Reverse transcription quantitative

Total RNA isolated from tobacco seedlings, leaves or hairy roots using RNeasy Plant Mini Kit (QIAGEN, Germantown, MD, USA) was used for cDNA synthesis and reverse transcription quantitative (RT-qPCR), as previously described [17]. The $2^{-\Delta\Delta CT}$ (cycle threshold) method was used to quantify gene expression. The tobacco *elongation factor1α* (*EF1α*; GenBank accession number D63396) and *α-tubulin* (GenBank accession number AJ421411) were used as internal controls [27]. The primers used in RT-qPCR are listed in Table S2.

2.7. Agrobacterium infiltration of N. benthamiana leaves, western blot, and phos-tag assay

For transient expression, a constitutively active form of *NtMAPKK2a*$^{T220D/T226D}$ fused to enhanced *GFP* (*eGFP*) was cloned in *pCAMBIA2301* containing the *CaMV 35S* promoter and *rbcS* terminator. *NtMPK4* fused to a 3× FLAG epitope was cloned in *pCAMBIA2301* with the *CaMV35S* promoter and *rbcS* terminator. *A. tumefaciens* GV3101 cells harboring *pCAMBIA2301-NtMPK4-FLAG* were infiltrated alone or in combination with *pCAMBIA2301-NtMPKK2a*^{DD}*-eFGP* into four-week-old *N. benthamiana* leaves. Leaf samples were collected 48 h after infiltration, and total proteins were extracted using extraction buffer containing 10% glycerol, 25 mmol L^{-1} Tris-Hcl, pH 7.5, 150 mmol L^{-1} NaCl, and Protease inhibitor cocktail (ThermoFisher Scientific, Waltham, MA, USA). Western blotting was performed using anti-FLAG-M2 (Sigma, St. Louis, MO, USA; Cat # F3165) and anti-GFP (ThermoFisher Scientific, USA; Cat # MA1-052) antibodies to detect the NtMPK4-FLAG and NtMPKK2a^{DD}-eGFP proteins, respectively. The SuperSep PHOS-tag gel (FULI FILM Wako, Osaka, Japan; Cat # 19517991) was used to separate the phosphorylated NtMPK4-FLAG protein, followed by western blotting using Anti-FLAG-M2 (Sigma; Cat # F3165) antibody, according to the manufacturer's protocol.

2.8. Promoter assays

For promoter assays, the *NtPMT* promoter (1.5 kb; −1499 to −1 numbered from the first ATG) was cloned in a vector containing the *GUS* reporter and *rbcS* terminator. The effector plasmids were made by cloning *NtERF221, NtMPKK2a, NtMPKK2b*, and *NtMEKK1b* into a modified pCAMBIA-1300 vector under the control of the *CaMV*35S promoter and *rbcS* terminator. The fire fly luciferase (*LUC*) gene driven by the *CaMV*35S promoter and *rbcS* terminator was used as an internal control. The vectors were transformed into *A. tumefaciens* strain GV3101 for infiltration. *A. tumefaciens* strain GV3101 harboring the binary vector of interest was grown overnight at 28 °C in LB medium supplemented with rifampicin and kanamycin. Bacterial cultures were centrifuged at 4000×*g* for 10 min and resuspended in infiltration buffer containing 10 mmol L^{-1} MES, 10 mmol L^{-1} $MgCl_2$, and 100 μmol L^{-1} acetosyringone. The optical density at 600 nm (OD_{600}) was adjusted to 0.5. The suspension was incubated at room temperature for 3 h before infiltration. Four-week-old *N. benthamiana* plants were used for infiltration. The bacterial suspension was infiltrated into the abaxial side of the leaves using a 1-mL needleless syringe. For co-infiltration experiments, equal volumes of different *Agrobacterium* cultures were mixed before application. Plants were kept under dark for 48 h. Samples were collected at designated time points post-infiltration for downstream analyses. Leaf protein extracts were used for determination of the LUC and GUS activity. Each experiment was repeated three times.

2.9. Vector construction and luciferase complementation imagine assay

For luciferase complementation imaging (LCI) assay, *NtMEKK1b*, *NtMPKK2a*, or *NtMPK4* were cloned into *pCAMBIA1300-NLuc*, *pCAMBIA1300-CLuc*, or *pCAMBIA1300-CCLuc* vectors [28]. The plasmids were transformed into *A. tumefaciens* GV3101 and then were co-infiltrated into *N. benthamiana* leaves and kept in dark. After 48 h, the leaves were infiltrated with luciferin, incubated for 10 min, then the leaves were collected and visualized using Azure Biosystem Imaging.

2.10. Alkaloid extraction and analysis

Nicotine content in hairy roots and tobacco leaves overexpressing or knocking down *NtMPKK2a* and *NtMEKK1b* and control was measured using gas chromatography with flame ionization detectors (GC-FID; PerkinElmer, Waltham, MA, USA; [29]). Nicotine content was reported as mg g^{-1} on a dry weight basis.

3. Results

3.1. Genome-wide identification of NtMAPKKs

MAPK cascades are essential signaling modules composed of at least three core components, a MAPKKK, a MAPKK, and a MAPK. MAPKKs are characterized by a conserved S/T- $X_{3\text{-}5}$-S/T motif (X represents any amino acid), which is phosphorylated by upstream MAPKKK, and the phosphorylated MAPKK then transmits the signals by phosphorylating downstream MAPK. In a previous study [17], *NtMPK4* has been shown to positively regulates nicotine biosynthesis. In Arabidopsis, the *MAP Kinase Kinase 2 (AtMKK2)* functions upstream of *MPK4* in the regulation of camalexin biosynthesis [30]. Based on these findings, we hypothesized that a tobacco homolog of *MAPKK2* acts upstream of *NtMPK4* and contributes to the regulation of nicotine biosynthesis. To test this hypothesis, we identified ten *NtMAPKK* sequences from tobacco genome and retrieved ten *AtMAPKK* sequences from TAIR (https://www.arabidopsis.org/). Phylogenetic analysis (Fig. 1B) revealed that two tobacco sequences, Nitab4.5_0002642g0020.1 and Nitab4.5_0002824g0020.1, clustered with *AtMPKK1/2*. We designated these two tobacco genes as *NtMPKK2a* and *NtMPKK2b*, respectively. Amino acid sequence alignments among *NtMPKK2a*, *NtMPKK2b*, and *AtMKK2* (Fig. S1) showed that both tobacco candidates share high sequence identity with *AtMPKK2,* with only one amino acid difference between *NtMPKK2a* and *NtMPKK2b*.

3.2. NtMPKK2a co-expresses with nicotine pathway genes and is inducible by JA

Nicotine biosynthesis occurs primarily in roots and is strongly inducible by JA [31]. Structural genes involved in the nicotine pathway, such as *NtPMT, NtQPT, NtA622, NtBBL*, as well as key TF genes

including *NtERF189, NtERF199, NtERF221,* are preferentially expressed in roots [5,17]. To determine the spatial expression patterns of *NtMPKK2s*, we performed a co-expression analysis using publicly available transcriptomic data (Accession no. PRJNA208209) across different tobacco tissues. As shown in Fig. 1C, *NtMPKK2a* exhibited significantly higher expression in roots compared to *NtMPKK2b*. Next, we analyzed the expression of nicotine pathway genes and *NtMPKK2a* in tobacco roots treated with JA. As shown in the Fig. 1D, *NtMPKK2a* expression was rapidly induced within 0.5 h of JA treatment, similar to the known regulators such as *ERF221*, *ERF189*, and *MYC2*, and then declined with prolonged exposure. In contrast, *NtMPKK2b* expression decreased following JA treatment. Taken together, despite differing by only a single amino acid, *NtMPKK2a* and *NtMPKK2b* display distinct expression patterns across tissues and in response to JA. *NtMPKK2a* is preferentially expressed in roots, inducible by JA, and co-expressed with key nicotine biosynthetic genes, suggesting a functional role in nicotine biosynthesis.

3.3. NtMPKK2a interacts with and phosphorylates NtMPK4

To determine whether NtMPKK2a and NtMPKK2b can directly interact with NtMPK4, we first performed yeast two-hybrid (Y2H) assay. *NtMPK4* was fused to the GAL4 DNA-binding domain (*GAL4-BD*) vector and co-transformed into yeast cells with activation domain (AD) constructs carrying *NtMPKK2a, NtMPKK2b,* or an empty vector as a negative control. Yeast cells expressing either *NtMPKK2a* or *NtMPKK2b* with *NtMPK4*, but not those with the control vector (Fig. 2A), grew on the selection medium lacking His, Leu, and Trp (−His/-Leu/-Trp), indicating that both NtMPKK2a and NtMPKK2b physically interact with NtMPK4. Given that NtMPKK2a and NtMPKK2b differ by only a single amino acid, we selected *NtMPKK2a* for further *in planta* validation. To confirm the interaction *in planta*, we performed a luciferase complementation imaging (LCI) assay by agroinfiltration of *N. benthamiana* leaves with constructs expressing *NtMPKK2a* and *NtMPK4* fused to N- and C-terminal luciferase fragments, respectively (Fig. 2C). Strong luminescence signals were observed in positive controls, *pNL-BREVE* and *pCL-CrICE1* [32], as well as in leaves co-expressing *NtMPKK2a* and *NtMPK4*, whereas no signal was detected in the negative control (Fig. 2D). These results confirm that NtMPKK2a and NtMPK4 interact *in planta*, likely having an enzyme-substrate relationship.

To identify the interaction interface between NtMPKK2a and NtMPK4, we performed AlphaFold-based structural modeling, and visualized the predicted complex using PyMOL. As shown in Fig. 2B, Glycine 222 (G222) of *NtMPKK2a* and Glutamate 199 (E199) of *NtMPK4* appear to form a covalent bond, suggesting a stable physical interaction. Notably, E199 within the TEY activation loop of NtMPK4 positioned adjacent to the critical phosphorylation sites T198 and Y200, potentially serving as a structural bridge for phosphate transfer during kinase activation. To determine whether NtMPKK2a can phosphorylate NtMPK4, we carried out *in vivo* phos-tag assay by transiently expressing *NtMPKK2a^{DD}-eGFP* (a phospho-mimic mutant of *NtMPKK2a,* in which T220/T226 were mutated to D) [33] along with *NtMPK4-FLAG*, either individually or in combination, in *N. benthamiana* leaves. Phosphorylation of *NtMPK4* was detected only when co-expressed with NtMPKK2a^{DD} (Fig. 2E, F), suggesting that activated NtMPKK2a is capable of phosphorylating NtMPK4 *in planta*.

3.4. Knockdown of NtMPKK2s suppresses nicotine biosynthesis in tobacco hairy roots

Given that nicotine is synthesized in tobacco roots and that *NtMPKK2a* is highly expressed in root tissues, we used hairy roots system to investigate the functional role of *NtMPKK2a*. Due to the high sequence similarity between *NtMPKK2a* and *NtMPKK2b*, both genes were targeted simultaneously using RNA interference (RNAi) in transgenic hairy roots. We selected two independent RNAi lines in which the transcript levels of *NtMPKK2*s were reduced over 50% for further analysis. The transgenic status was validated by PCR (Fig. S2A). To examine the effects of *NtMPKK2*s silencing on the nicotine pathway genes, we performed RT-qPCR on RNA isolated from the two RNAi lines and EV roots (Fig. 3A). The results showed that expression of key nicotine pathway genes such as *NtPMT, NtQPT, NtBBL,* and a nicotine transporter *NtMATE1*, was decreased by 40% to 75% in the RNAi lines. Expression of *BBLa* was measured in this study. Because *BBL* genes share high sequence homology; *BBLa* and *BBLc* share approximately 90% sequence identity, we thus refer to them collectively as 'BBL'. Among the key TFs, *NtERF189* transcript levels were significantly decreased to 45%–55% of control levels, whereas *NtMYC2* and *NtERF221* expression remained unchanged. Consistently, nicotine contents in the two RNAi lines reduced approximately 20%–30% compared to control (Fig. 3B), suggesting the knockdown of *NtMPKK2s* negatively affects nicotine biosynthesis.

3.5. NtMPKK2a overexpression induces nicotine biosynthesis in tobacco hairy roots

To further substantiate the effects of *NtMPKK2a* on nicotine biosynthesis, we generated transgenic tobacco hairy roots overexpressing *NtMPKK2a* under the control of a dexamethasone (DEX)-inducible promoter. Multiple transgenic lines were obtained and transgenic status of two selected lines was confirmed by PCR (Fig. S2B). Following DEX induction, two lines exhibiting *NtMPKK2a* expression levels 4- to 6-fold higher than those in uninduced controls were selected for gene expression and nicotine content analysis. Expression of nicotine pathway genes such as *NtPMT*, *NtA622*, and *NtBBL*, as well as key TF such as *NtERF189* was 1.5–2-fold higher compared to control (Fig. 4A). To determine whether *NtMPKK2a* overexpression influences nicotine accumulation, we quantified the nicotine contents in the two selected lines (Fig. 4B). Both transgenic lines showed a moderate but significant increase in nicotine content compared to their uninduced controls, supporting a positive regulatory role for *NtMPKK2a* in nicotine biosynthesis.

3.6. NtMPKK2s enhance the transactivation activity of NtERF221 on the NtPMT promoter in planta

NtMPK4 is known to enhance the transactivation activity of *NtERF221* on nicotine pathway gene promoters in tobacco cells [17]. We hypothesized that, as an upstream kinase of *NtMPK4, NtMPKK2a* may similarly enhances the *NtERF221*-mediated transactivation of nicotine pathway genes. To test our hypothesis, we performed a *N. benthamiana* leaf-based promoter assays using agroinfiltration. A construct containing the *NtPMT* promoter fused to a GUS reporter gene was infiltrated into *N. benthamiana* leaves either alone (control) or in combination with *NtERF221* and *NtMPKK2a* as effectors. *NtERF221* alone increased *NtPMT* promoter activity by approximately 11-fold. Co-infiltration with *NtERF221* and *NtMPKK2a* further enhanced promoter activity to 19-fold and 18-fold, respectively (Fig. 4C). These results indicate that both *NtMPKK2a* enhanced the transactivation activity of *NtERF221* on the *NtPMT* promoter *in vivo*, possibly via the phosphorylation of endogenous NbMPK4.

3.7. Genome-wide identification and sequence alignments of NtMEKK1s

*MAPKKK*s are classified into three subfamilies: MAPK ERK kinase kinase (MEKK), zipper interacting protein kinase (ZIK), and

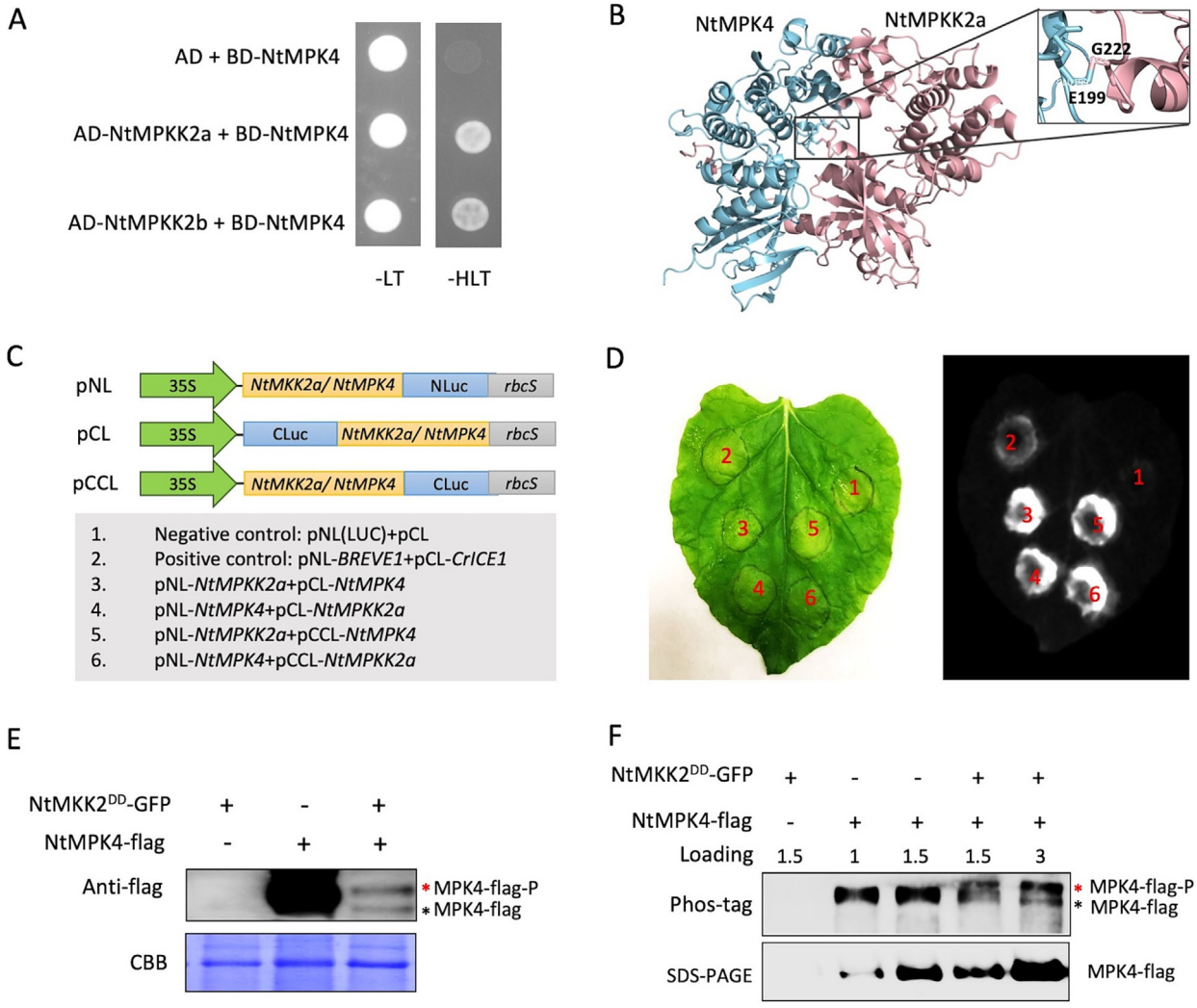

Fig. 2. NtMPKK2a interacts with and phosphorylates NtMPK4. (A) NtMPKK2a and NtMPKK2b interact with NtMPK4 in yeast cells. AD-NtMPKK2a + BD and AD-NtMPKK2b + BD did not grow on selection medium and thus were not included in the figure. (B) AlphaFold 3.0 structural modeling of the interaction between NtMPK4 and NtMPKK2a. The interaction sites between G222 in NtMPKK2a and E199 in NtMPK4 was enlarged. (C) Schematic diagrams of the vectors used in Luciferase complementation imaging (LCI) assay. (D) LCA shows NtMPKK2a interacts with NtMPK4 in plant cells. 1, negative control: *pNL* (*LUC*) + *pCL*; 2, positive control: *pNL-BREVE1* + *pCL-CrICE1*; 3, *pNL-NtMPKK2a* + *pCL-NtMPK4*; 4, *pNL-NtMPK4* + *pCL-NtMPKK2a*; 5, *pNL-NtMPKK2a* + *pCCL-NtMPK4*; 6, *pNL-NtMPK4* + *pCCL-NtMPKK2a*. (E) The constitutively active NtMPKK2a^{DD} phosphorylates NtMPK4 *in vivo*. *NtMPK4-FLAG* alone or in combination with *NtMPKK2a^{DD}-eGFP* was transiently expressed in *N. benthamiana* leaves. The proteins were separated on a Phos-tag gel, and detected using anti-FLAG antibodies. The phosphorylated (MPK4-FLAG-P; upper band) and unphosphorylated (MPK4-FLAG; lower band) NtMPK4 showed differential migration on a Phos-tag gel. The Coomassie Brilliant Blue R-250 (CBB) stained Rubisco is used as the loading control. (F) The phos-tag assay showing the constitutively active NtMPKK2a^{DD} phosphorylates NtMPK4. *NtMPK4-FLAG*, alone or in combination with *NtMPKK2a^{DD}-eGFP*, was transiently expressed in *N. benthamiana* leaves. Proteins were separated on a Phos-tag gel and detected using anti-FLAG antibodies. A conventional SDS-PAGE Western blot of NtMPK4-flag served as a loading control. The numbers (1, 1.5, 3) indicate relative loading amounts, adjusted according to the protein levels produced.

rapidly accelerated fibrosarcoma (Raf) families [34]. The tobacco genome harbors over 150 *MAPKKKs,* of which 38 belong to the *MEKK* subfamily [22]. To identify potential *NtMEKK1* candidates, we constructed a phylogenetic tree using 38 tobacco MEKKs and 21 *Arabidopsis* MEKKs (Fig. 5A). The analysis revealed 3 tobacco *MEKK1* candidates clustering closely with *AtMEKK1*, which we designated as *NtMEKK1a* (Nitab4.5 0004005 g0030.1), *NtMEKK1b* (Nitab4.5 0004360 g0030.1), and *NtMEKK1c* (Nitab4.5 0006653 g0040.1). Multiple sequence alignments (Fig. 5B) showed that *AtMEKK1* shared 47.7% identity with *NtMEKK1a*, 51% with *NtMEKK1b*, and 50.71% with *NtMEKK1c*. *NtMEKK1b* and *NtMEKK1c* are highly similar, with approximately 94% sequence identity, while the *NtMEKK1a* more distantly related to the other two. Notably, the C-terminal kinase domains are highly conserved among the candidates, suggesting functional similarity in catalytic activity. In contrast, the N-terminal regulatory regions are more divergent, potentially reflecting differences in regulatory interactions or subcellular localization.

3.8. NtMEKK1b interacts with NtMPKK2a

In *Arabidopsis*, MEKK1 functions as the upstream component in the MEKK1-MKK2-MPK4 cascade [35,36]. Based on this, we hypothesized that the authentic NtMEKK1 in tobacco would interact with NtMPKK2a. To investigate which of the three NtMEKK1 candidates interacts with NtMPKK2a, we performed Y2H assays. As shown in Fig. 5C, among the three candidates, only the yeast strain co-expressing *pBD-NtMEKK1b* and *pAD-NtMPKK2* grew on the selection medium (–AHLT), indicating a specific interaction between NtMEKK1b and NtMPKK2a. We then performed AlphaFold-based protein–protein interaction (PPI) prediction of NtMEKK1b and NtMPKK2a. As shown in Fig. 5D, the predicted interface (cyan

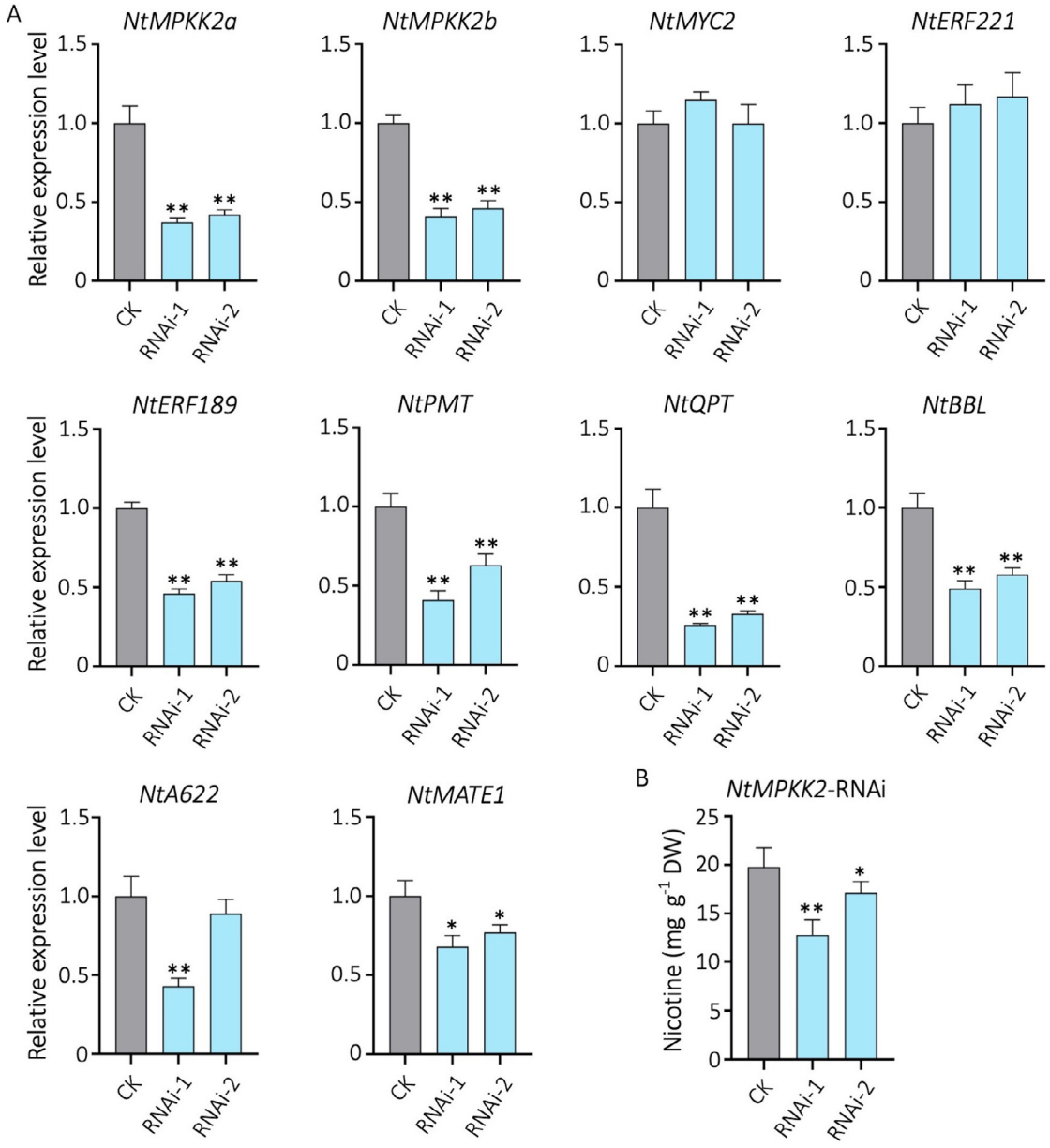

Fig. 3. Expression analysis of nicotine pathway genes and measurement of nicotine contents in *NtMPKK2s-RNAi* hairy roots. (A) Relative expression of *NtMPKK2s* and nicotine pathway genes in CK (control, empty vector) and two *NtMPKK2-RNAi* hairy root lines was determined by RT-qPCR. *EF1α* was used as an internal control for normalization. (B) Nicotine contents in *CK* and *MPKK2-RNAi* lines were determined by GC-FID. Statistical significance was calculated using the Student's *t*-test: *, $P < 0.05$; **, $P < 0.01$.

regions) represents areas where atoms from both proteins are within 4Å, a commonly accepted threshold for molecular interaction. The model revealed over 400 atoms within 4Å and 223 atoms within 3 Å, but no atoms within 2Å, suggesting that the interaction between NtMEKK1b and NtMPKK2a is transient and flexible rather than covalent or tightly bound. We further mapped potential catalytic and phosphorylation sites involved in the interaction. Predicted kinase active sites in *NtMEKK1b* (marked in red) and possible phosphorylation sites in *NtMPKK2a* (marked in yellow) were all located within 4Å of the interface. Finally, lysine 447 (K447) and glutamate 492 (E492) in NtMEKK1b were found in close proximity to threonine 226 (T226) and threonine 220 (T220) in NtMPKK2a, respectively (Fig. 5E, F). The distance between NtMEKK1b^{K447}-NtMPKK2a^{T226} and NtMEKK1b^{E492}-NtMPKK2a^{T220} were approximately 7.6 Å, suggesting that these catalytic sites are well-positioned for phosphorylation activity but are not involved in forming a stable dimeric complex.

3.9. RNAI-mediated silencing of NtMEKK1b reduces nicotine accumulation in transgenic tobacco plants

To verify the function of *NtMEKK1b* in nicotine biosynthesis, we generated *NtMEKK1b*-RNAi transgenic tobacco plants. Two independent lines (*RNAi-1* and *RNAi-6*) were selected, showing 34% and 80% reductions in *NtMEKK1b* expression, respectively. The transgenic status was confirmed by PCR (Fig. S3A). The RNAi lines were phenotypically similar to the control plants (Fig. S4A, B). We further performed RT-qPCR to measure the expression of key nicotine pathway genes and determined nicotine contents in the transgenic lines. As shown in Fig. 6A, silencing of *NtMEKK1b* resulted in significant downregulation of multiple nicotine pathway genes, with *NtPMT*, *NtA622*, and *NtBBL* transcripts reduced by 90%–99%. Expression of key TFs *NtERF189* and *NtERF221* also significantly decreased. Consistent with the transcriptional changes, both RNAi lines exhibited a moderate but significant reduction in nicotine

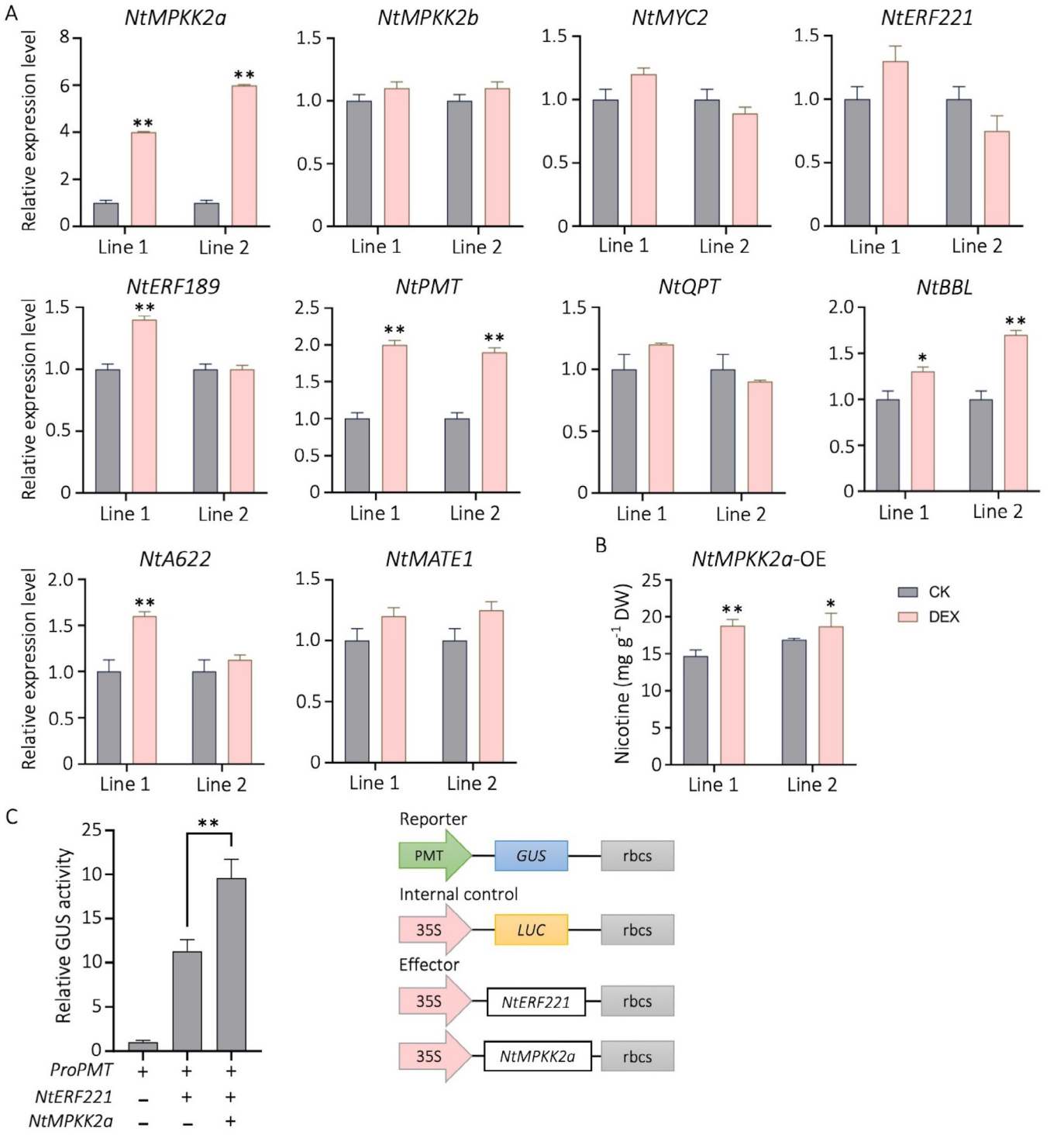

Fig. 4. Expression analysis of nicotine pathway genes and measurement of nicotine contents in *NtMPKK2s* overexpressing tobacco hairy roots. (A) Relative expression of *NtMPKK2s* and nicotine pathway genes in two pTA-NtMPKK2a lines, uninduced-hairy roots were used as control (CK) and two DEX-induced *NtMPKK2a* lines were used as overexpression hairy root lines. The CK represents uninduced-control, the DEX represents DEX-induced overexpression lines (Line 1 and Line 2). Relative expression was determined by RT-qPCR. *EF1α* was used as an internal control for normalization. (B) Nicotine contents in *CK* and DEX-induced-*NtMPKK2a* overexpression lines were determined by GC-FID. (C) Co-expression of NtMPKK2a with NtERF221 significantly increased the *NtPMT* promoter (*proPMT*) activity in *N. benthamiana* leaves. pro*PMT* fused to the *GUS* reporter was co-infiltrated into *N. benthamiana* leaves alone or with the effector plasmids expressing *NtERF221*, and *NtMPKK2a*. A plasmid containing *CaMV35S*-firefly *luciferase* (*LUC*) served as an internal control. GUS activity was normalized against the LUC activity. Values are means ± SD of three biological samples. Statistical significance was calculated using the Student's *t*-test: *, $P < 0.05$; **, $P < 0.01$.

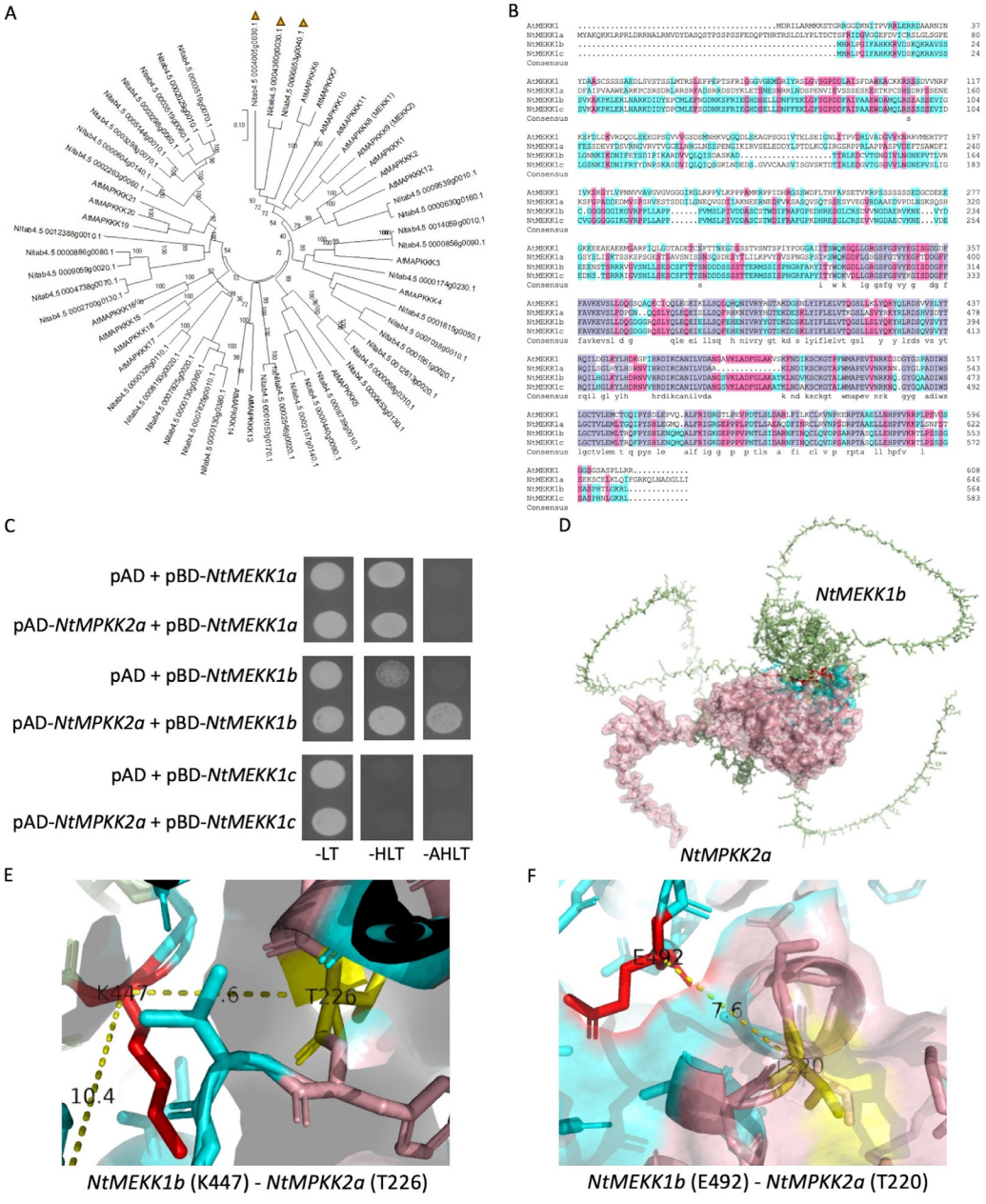

Fig. 5. Identification, phylogenetic analysis, structural modeling, protein–protein interaction of *NtMEKK1b*. (A) Phylogenetic tree of *MEKK* subfamily genes from tobacco and *Arabidopsis*. Nitab4.5 0004005 g0030.1, Nitab4.5 0004360 g0030.1, and Nitab4.5 0006653 g0040.1 were clustered with *AtMEKK1* and designated as *NtMEKK1a*, *NtMEKK1b*, and *NtMEKK1c*, respectively. The three candidates are indicated by triangles. (B) Amino acid sequence alignments of *NtMEKK1a*, *NtMEKK1b*, *NtMEKK1c*, and *AtMEKK1*. (C) *NtMEKK1b* interacts with *NtMPKK2a* in yeast. *pBD-NtMEKK1a/b/c* was co-transformed either with *pAD-NtMPKK2a* or with empty *pAD* vector as control. (D) AlphaFold 3.0 modeling of the interaction between *NtMEKK1b* and *NtMPKK2a*. The green chain represents *NtMEKK1b*, whereas the pink chain represents *NtMPKK2a*, and the cyan parts indicate the interface residues (< 4 Å). The red colored residues are Asp (D), Glu (E), Lys (K), Arg (R), His (H) in *NtMEKK1b* and close to *NtMPKK2a* (< 4 Å), indicating putative kinase active sites. The yellow-colored residues are Ser (S), Thr (T) in *NtMPKK2a* and close to *NtMEKK1b* (< 4 Å), indicating putative phosphorylation sites. (E) The distance between the catalytic site (K447) in NtMEKK1b and phosphorylation site (T226). (F) The distance between the catalytic site (E492) and the phosphorylation site (T220) in NtMPKK2a. Both catalytic sites in NtMEKK1b, K447 and E492, are conserved among the three candidates and AtMEKK1.

content (Fig. 6C), suggesting a positive regulatory role of *NtMEKK1b* in nicotine biosynthesis through post-translational modification.

3.10. Overexpression of NtMEKK1b induces nicotine biosynthesis in tobacco hairy roots

To further explore the function of *NtMEKK1b* in regulating nicotine biosynthesis, we generated DEX-inducible *NtMEKK1b*-overexpression hairy roots. Following DEX treatment, we analyzed the expression of nicotine pathway genes and measured nicotine content. As *NtMEKK1b* functions upstream of *NtMPKK2a* in the same MAPK cascade, we anticipated similar regulatory effects to those observed in *NtMPKK2a*-overexpressing lines. We selected two lines, line 1 and line 2, in which *NtMEKK1b* expression increased by 34% and 87% upon DEX induction, respectively. Besides, transgenic status of both lines was verified by PCR (Fig. S3B). RT-qPCR analysis revealed significant upregulation of several nicotine biosynthetic genes (Fig. 6B). TFs *NtERF189* and *NtERF199* were upregulated by 50%–200%, while structural genes *NtQPT* and *NtPMT* increased by 83%–282%. Additional genes,

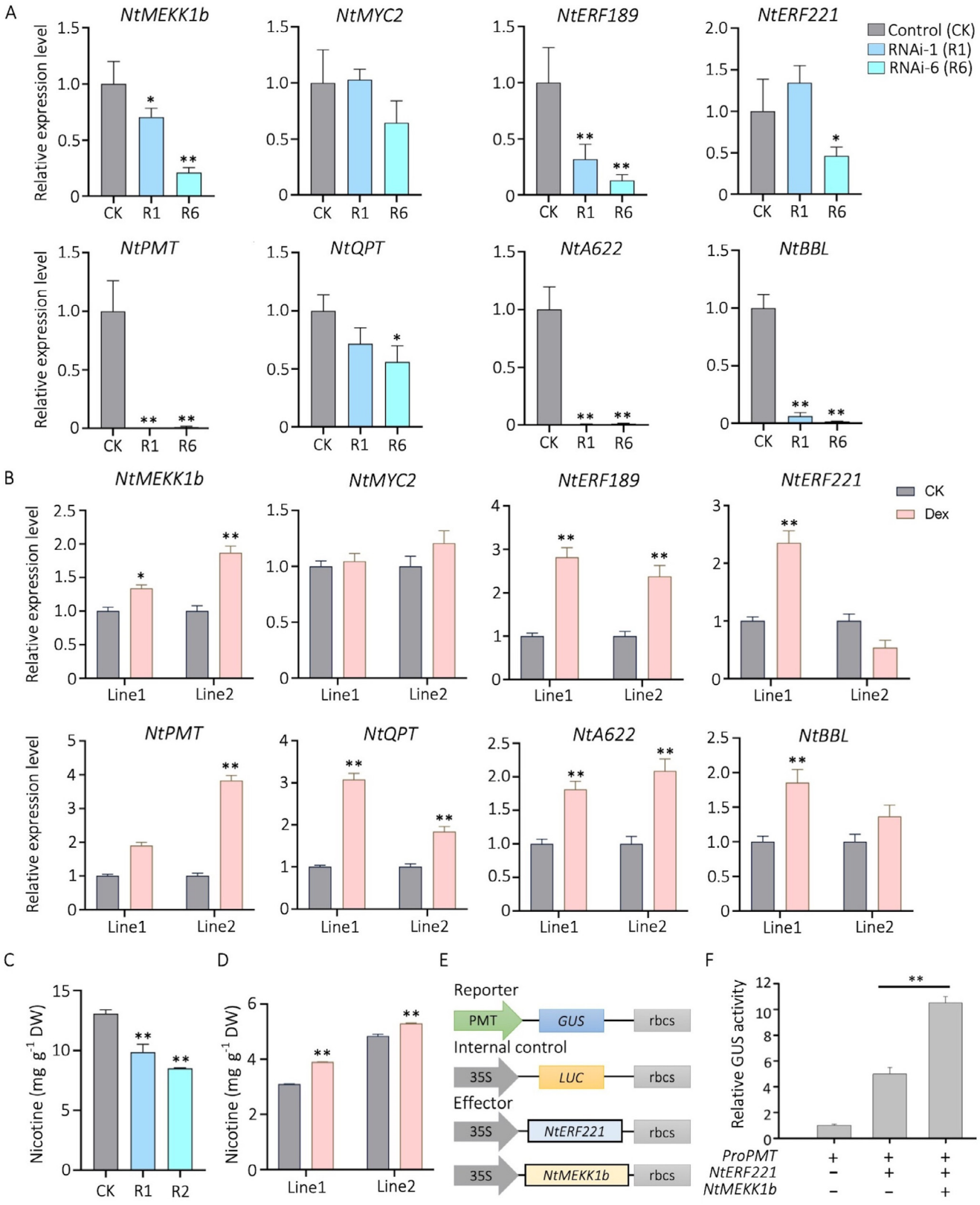

Fig. 6. Expression analysis of nicotine pathway genes and measurement of nicotine contents in *NtMEKK1b RNAi* plants and overexpressing hairy roots. (A) Relative expression of key nicotine pathway genes in RNAi plants. *EF1α* was used as an internal control for normalization. (B) Relative expression of *NtMEKK1b* and nicotine pathway genes in two *pTA-NtMEKK1b* hairy root lines under uninduced control (CK) and DEX-induced conditions. CK represents uninduced-controls, and DEX represents DEX-induced overexpression lines (Line 1 and Line 2). Relative expression was determined by RT-qPCR, With *EF1α* used as an internal control for normalization. (C) Nicotine contents in control (*EV*) and two *NtMEKK1b-RNAi* lines (RNAi-1 and RNAi-6) measured using GC-FID. (D) Nicotine contents in CK and DEX-induced-*NtMEKK1b* overexpression lines, measured using GC-FID. (E) Schematic diagrams of the constructs used for *N. benthamiana* leaf infiltration assay. (F) Co-expression of *NtMEKK1b* with *NtERF221* significantly increased *NtPMT* promoter (*proPMT*) activity in *N. benthamiana* leaves. pro*PMT* fused to the *GUS* reporter was co-infiltrated alone or with effector plasmids expressing *NtERF221*, *NtMEKK1b*, or both. A plasmid containing *CaMV35S*- firefly *luciferase* (*LUC*) served as an internal control. GUS activity was normalized to LUC activity. Statistical significance was calculated using the Student's *t*-test: *, $P < 0.05$; **, $P < 0.01$.

including *NtBBL*, *Nt*A622, and *NtMATE1*, also exhibited induction compared to control. Consistent with gene expression data, both overexpression lines exhibited elevated nicotine content compared to the uninduced controls (Fig. 6D), supporting the conclusion that *NtMEKK1b* positively regulates nicotine biosynthesis.

3.11. NtMEKK1b enhances the transactivation activity of NtERF221 on the NtPMT promoter

Because *NtMPKK2a* enhances transcriptional activation of *NtERF221* on the *NtPMT* promoter, we hypothesized that *NtMEKK1b* can also enhance *NtERF221* transcriptional activity on the *NtPMT* promoter. To test this, we performed a *N. benthamiana* leaf-based promoter transactivation assay. The *NtPMT* promoter was fused to a GUS reporter gene, while the *pCAMBIA-LUC* vector served as an internal control for normalization. Constructs expressing either *NtERF221* alone or *NtERF221* in combination with *NtMEKK1b* were transiently co-infiltrated into *N. benthamiana* leaves (Fig. 6E). *NtERF221* alone increased *NtPMT* promoter activity by approximately five-fold. When co-expressed with *NtMEKK1b*, promoter activity was further enhanced to ten-fold ($P < 0.01$), confirming that *NtMEKK1b* significantly boosts *NtERF221*-mediated transactivation of the *NtPMT* promoter (Fig. 6F). These results support the role of *NtMEKK1b* as a positive modulator of nicotine biosynthesis through enhancement of transcription factor activity.

3.12. NtMEKK1b is phosphorylated in response to JA and flg22 treatments

As the most upstream component of the NtMEKK1b-NtMPKK2a-NtMPK4 signaling cascade, NtMEKK1b is a likely target of phosphorylation by various external stimuli. In Arabidopsis, *MEKK1* participates in at least two distinct cascade, MEKK1-MKK4/5-MPK3/6 [37] and MEKK1-MKK1/2-MPK4 [35]. Given that *NtMEKK1b* is transcriptionally induced by JA and that Arabidopsis *MEKK1* is activated by the flagellin-derived peptide flg22, we investigated whether JA and flg22 treatments also promote phosphorylation of *NtMEKK1b* in tobacco. To test this, we transiently expressed *NtMEKK1b* fused with a C-terminal FLAG tag in *N. benthamiana* leaves via *Agrobacterium tumefaciens* strain GV3101. Following infiltration, leaves were treated with 100 μmol L^{-1} methyl jasmonate (MeJA), 1 μmol L^{-1} flg22, or mock solution. Protein extracts were analyzed by Phos-tag SDS-PAGE to assess phosphorylation status. Interestingly, even mock-treated controls, *NtMEKK1b* displayed two phosphorylation bands, suggesting that the protein undergoes autophosphorylation (Fig. 7A). However, MeJA or flg22 treatment triggered additional phosphorylation suggesting that both JA and flg22 serve as upstream signals that enhance the phosphorylation and potentially the activation of *NtMEKK1b*.

4. Discussion

This study sets out to elucidate the upstream signaling mechanisms regulating nicotine biosynthesis in tobacco, focusing on the post-translational control mediated by a MAPK signaling cascade. Our overarching hypothesis was that a canonical MAPK module, composed of a MAP kinase kinase kinase (*NtMEKK1b*), a MAP kinase kinase (*NtMPKK2a*), and a MAP kinase (*NtMPK4*), regulates nicotine biosynthesis in response to environmental biotic signals such as JA and the bacterial elicitor flg22. While previous studies have highlighted the transcriptional regulation of nicotine pathway genes by JA-responsive TFs [6,38], the post-translational mechanisms that fine-tune these responses remain poorly understood. Our work bridges this knowledge gap by identifying and functionally characterizing a MAPK cascade that directly links extracellular stimuli to the modulation of TF activity and downstream alkaloid biosynthesis.

We began by identifying *NtMPKK2a* as a candidate upstream kinase of *NtMPK4*, based on sequence homology with *Arabidopsis MKK2*, a kinase known to regulate defense-related secondary metabolism [30]. *NtMPKK2a* is preferentially expressed in tobacco roots, where nicotine biosynthesis occurs, and is strongly induced by JA treatment (Fig. 1). Phylogenetic and transcriptomic analyses revealed that *NtMPKK2a* is co-expressed with key nicotine biosynthetic genes and JA-responsive TFs, supporting a regulatory role (Fig. 1). Importantly, NtMPKK2a physically interacts with NtMPK4 in yeast and *in planta*, and phosphorylation assays confirmed that NtMPKK2a directly phosphorylates NtMPK4 (Fig. 2). Functional studies using RNAi-mediated silencing and DEX-inducible overexpression of *NtMPKK2a* in hairy roots (Figs. 3, 4) demonstrated that *NtMPKK2a* positively regulates the expression of nicotine biosynthetic genes and nicotine accumulation. These findings establish *NtMPKK2a* as a key intermediate in the nicotine biosynthesis signaling cascade.

In a previous study, another MAPKK, *NtMAPKK1* (*JAM1*) was identified in tobacco and shown to enhance the *trans*-activity of *NtORC1* (*NtERF221*) on *NtPMT2* and *NtQPT2* promoter after JA treatments [10]. Similarly, our study also proved NtMPKK2a enhances the transcriptional activation of *NtERF221*, a NIC2-locus TF critical for JA-induced nicotine biosynthesis (Fig. 4C). Transactivation assays showed that co-expression of *NtMPKK2a* with *NtERF221* significantly increased *NtPMT* promoter activity. This suggests that NtMPKK2a, through NtMPK4-mediated phosphorylation, modulates the activity of downstream TFs, providing mechanistic insight into how signal transduction intersects with transcriptional regulation in specialized metabolism.

The MAPK cascades normally possess at least three components. To identify the upstream regulator of NtMPKK2a, we performed genome-wide screening of tobacco MEKK genes and identified NtMEKK1b as the most likely candidate, based on sequence similarity to AtMEKK1, phylogenetic position, and interaction with NtMPKK2a in yeast. AlphaFold-based protein–protein interaction modeling further supported this interaction, revealing a close proximity between catalytic residues in NtMEKK1b and potential phosphorylation sites in NtMPKK2a. Although the interaction appeared transient, such flexibility is characteristic of many kinase-substrate relationships in signaling networks (Fig. 5).

Functional validation of *NtMEKK1b* supported its role in nicotine regulation. RNAi-mediated silencing of *NtMEKK1b* in stable transgenic plants led to dramatic reductions in the expression of nicotine pathway genes, including *NtPMT*, *NtBBL*, *NtA622*, and a key TF *NtERF189*, along with a significant decrease in nicotine content (Fig. 6A–C). Conversely, overexpression of *NtMEKK1b* in hairy roots significantly upregulated these genes and increased nicotine accumulation (Fig. 6B–D). Moreover, NtMEKK1b enhanced the transactivation activity of NtERF221 on the *NtPMT* promoter, further corroborating its regulatory function (Fig. 6F). These findings indicate that NtMEKK1b, like NtMPKK2a, contributes to nicotine biosynthesis through both transcriptional and post-translational mechanisms.

One of the most notable aspects of this study is the demonstration that NtMEKK1b is activated by multiple external stimuli. We showed that both MeJA and flg22 treatments enhanced NtMEKK1b phosphorylation in *N. benthamiana* leaves (Fig. 7A). While the control samples already exhibited basal phosphorylation, likely due to autophosphorylation, treatments with JA and flg22 triggered additional phosphorylation, suggesting that *NtMEKK1b* integrates hormonal and microbial signals. This is consistent with the dual role of *Arabidopsis MEKK1* in both JA-mediated and pathogen-triggered pathways, such as the *MEKK1-MKK1/2-MPK4* and

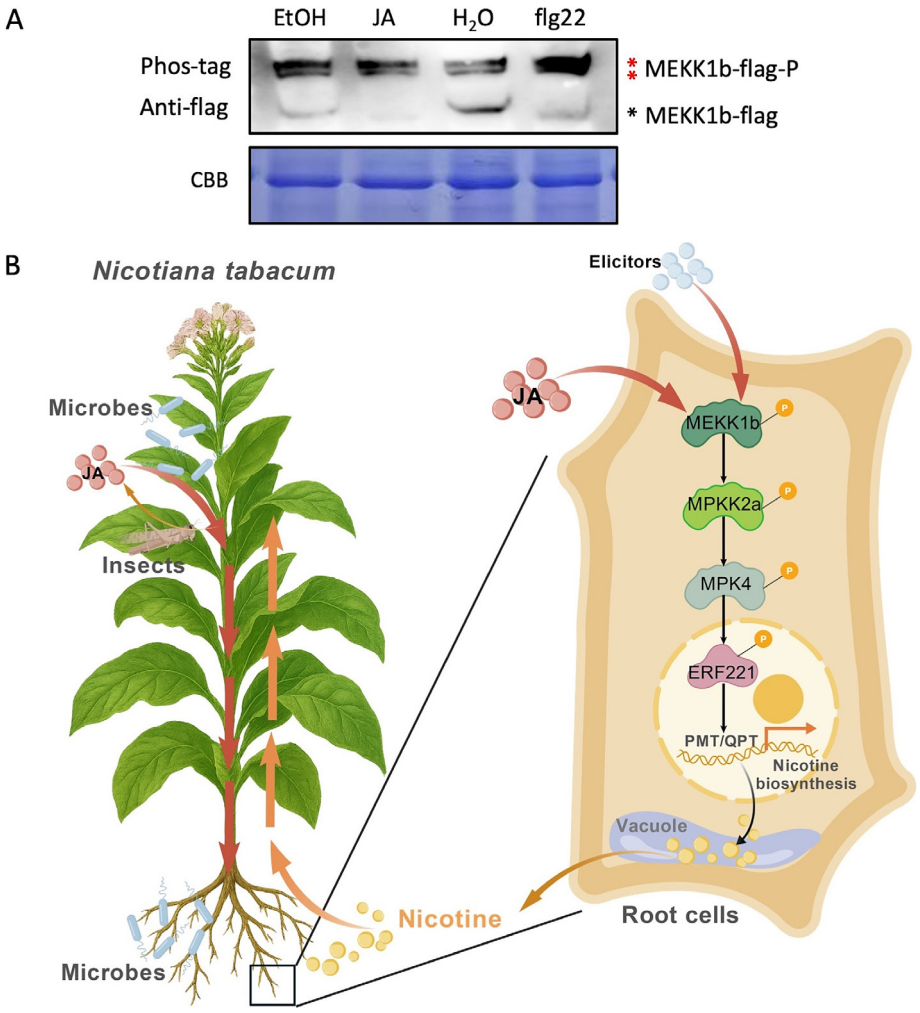

Fig. 7. NtMEKK1b is phosphorylated in response to flg22 or JA treatment. (A) NtMEKK1b is auto-phosphorylated and can be phosphorylated by JA and flg22 treatments. NtMEKK1b-FLAG was transiently expressed in *N. benthamiana* leaves. After MeJA and flg22 treatments, the protein was separated by phos-tag gel and incubated with anti-flag antibody. The coomassie brilliant blue (CBB) stained Rubisco is used as the loading control. (B) A schematic diagram showing the MAP Kinase cascade module NtMEKK1b-NtMPKK2a-NtMPK4 regulation of nicotine biosynthesis in tobacco. The insects and microbes elicit JA signaling and activate the NtMEKK1b-NtMPKK2a-NtMPK4 cascade and induce nicotine biosynthesis by enhancing the transactivation activity and expression of *ERF221* transcription factors and nicotine pathway genes.

MEKK1-MKK4/5-MPK3/6 modules [36,39]. Therefore, *NtMEKK1b* may serve as a signal integration node, allowing tobacco to fine-tune nicotine biosynthesis under various environmental conditions [40]. In Arabidopsis, MEKK1 contains an N-terminal regulatory domain (1–332 aa) and a C-terminal kinase domain, with the regulatory domain typically suppressing kinase activity [41]. Autophosphorylation of AtMEKK1 has been reported at Y204 and Y323 within the N-terminus region [42]. Additionally, a Ca^{2+}/calmodulin-regulated receptor-like kinase, CRLK1, also phosphorylates MEKK1 at its N-terminus, suggesting the complexity of MEKK1 activation [41].

Our findings have significant implications for both plant biology and agricultural biotechnology. First, this work underscores the importance of post-translational regulation in specialized metabolism, a relatively underexplored area compared to transcriptional control. Second, the identification of a MAPK cascade that modulates nicotine biosynthesis in response to biotic cues expands our understanding of how plants integrate environmental signals into metabolic outputs. Finally, from a practical perspective, targeting components of the NtMEKK1b-NtMPKK2a-NtMPK4 cascade could provide new strategies for developing low-nicotine tobacco varieties. Since direct suppression of biosynthetic genes or TFs has yielded only partial reductions in nicotine levels, modulating upstream signaling nodes may offer a more robust and tunable approach.

In summary, we uncovered a previously uncharacterized MAPK cascade, NtMEKK1b-NtMPKK2a-NtMPK4, that positively regulates nicotine biosynthesis in tobacco (Fig. 7B). This signaling module transduces external cues, including JA and pathogen-associated molecular patterns such as flg22, into post-translational modifications that enhance TF activity and nicotine pathway gene expression. Our study highlights the critical role of post-translational signaling in specialized metabolism and identifies new regulatory nodes with potential utility in metabolic engineering and harm reduction in tobacco.

CRediT authorship contribution statement

Yan Zhou: Writing – original draft, Validation, Investigation, Formal analysis, Data curation. **Yongliang Liu:** Investigation, Formal analysis, Data curation. **Ruiqing Lyu:** Investigation, Formal analysis. **Sanjay Kumar Singh:** Investigation, Formal analysis. **Xueyi Sui:** Formal analysis, Data curation. **Xin Hou:** Formal analysis, Data curation. **Sitakanta Pattanaik:** Writing – review & editing, Supervision, Project administration, Investigation, Funding acquisition, Conceptualization. **Ling Yuan:** Writing – review &

editing, Supervision, Resources, Project administration, Funding acquisition, Conceptualization.

Declaration of competing interest

The authors declare that they have no known competing financial interests or personal relationships that could have appeared to influence the work reported in this paper.

Acknowledgment

This work was supported partially by the Kentucky Tobacco Research and Development Center (KTRDC), University of Kentucky.

Appendix A. Supplementary data

Supplementary data for this article can be found online at https://doi.org/10.1016/j.cj.2025.08.012.

References

[1] S.A. Grando, Connections of nicotine to cancer, Nat. Rev. Cancer 14 (2014) 419–429.
[2] X. Wu, S.K. Singh, B. Patra, J. Wang, S. Pattanaik, L. Yuan, An overview of the regulation of specialized metabolism in tobacco, Curr. Plant Biol. 41 (2024) 100431.
[3] Y.X. Liu, W.H. Han, J.X. Wang, F.B. Zhang, S.X. Ji, Y.W. Zhong, S.S. Liu, X.W. Wang, Differential induction of JA/SA determines plant defense against successive leaf-chewing and phloem-feeding insects, J. Pest. Sci. 98 (2024) 1085–1100.
[4] L. Yuan, Clustered ERF transcription factors: not all created equal, Plant Cell Physiol. 61 (2020) 1025–1027.
[5] M. Kajikawa, N. Sierro, H. Kawaguchi, N. Bakaher, N.V. Ivanov, T. Hashimoto, T. Shoji, Genomic insights into the evolution of the nicotine biosynthesis pathway in tobacco, Plant Physiol. 174 (2017) 999–1011.
[6] T. Shoji, T. Hashimoto, K. Saito, Genetic regulation and manipulation of nicotine biosynthesis in tobacco: strategies to eliminate addictive alkaloids, J. Exp. Bot. 75 (2024) 1741–1753.
[7] R.E. Dewey, J. Xie, Molecular genetics of alkaloid biosynthesis in *Nicotiana tabacum*, Phytochemistry 94 (2013) 10–27.
[8] N. Burner, S.P. Kernodle, T. Steede, R.S. Lewis, Editing of A622 genes results in ultra-low nicotine whole tobacco plants at the expense of dramatically reduced growth and development, Mol. Breed. 42 (2022) 20.
[9] J.H. Jeong, E.Y. Jeon, Y.J. Song, M.K. Hwang, Y. Gwak, J.Y. Kim, Impact of CRISPR/Cas9-induced mutations in nicotine biosynthesis core genes A622 and BBL on tobacco: Reduction in nicotine content and developmental abnormalities, Curr. Plant Biol. 38 (2024) 100343.
[10] K. de Boer, S. Tilleman, L. Pauwels, R. Vanden Bossche, V. de Sutter, R. Vanderhaeghen, P. Hilson, J.D. Hamill, A. Goossens, APETALA2/ETHYLENE RESPONSE FACTOR and basic helix–loop–helix tobacco transcription factors cooperatively mediate jasmonate-elicited nicotine biosynthesis, Plant J. 66 (2011) 1053–1065.
[11] G. Manning, D.B. Whyte, R. Martinez, T. Hunter, S. Sudarsanam, The protein kinase complement of the human genome, Science 298 (2002) 1912–1934.
[12] M.D. Lehti-Shiu, S.H. Shiu, Diversity, classification and function of the plant protein kinase superfamily, Philos. Trans. R. Soc. B 367 (2012) 2619–2639.
[13] L.P. Hamel, M.C. Nicole, S. Sritubtim, M.J. Morency, M. Ellis, J. Ehlting, N. Beaudoin, B. Barbazuk, D. Klessig, J. Lee, Ancient signals: comparative genomics of plant MAPK and MAPKK gene families, Trends Plant Sci. 11 (2006) 192–198.
[14] M. Zhang, S. Zhang, Mitogen-activated protein kinase cascades in plant signaling, J. Integr. Plant Biol. 64 (2022) 301–341.
[15] Y. Zhou, S.K. Singh, B. Patra, Y. Liu, S. Pattanaik, L. Yuan, Mitogen-activated protein kinase-mediated regulation of plant specialized metabolism, J. Exp. Bot. 76 (2025) 262–276.
[16] R. Lyu, S.K. Singh, Y. Liu, B. Patra, Y. Zhou, B. Wang, S. Pattanaik, L. Yuan, Reprogramming plant specialized metabolism by manipulating protein kinases, aBIOTECH 2 (2021) 226–239.
[17] X. Liu, S.K. Singh, B. Patra, Y. Liu, B. Wang, J. Wang, S. Pattanaik, L. Yuan, Protein phosphatase NtPP2C2b and MAP kinase NtMPK4 act in concert to modulate nicotine biosynthesis, J. Exp. Bot. 72 (2021) 1661–1676.
[18] S. Pattanaik, Q. Kong, D. Zaitlin, J.R. Werkman, C.H. Xie, B. Patra, L. Yuan, Isolation and functional characterization of a floral tissue-specific R2R3 MYB regulator from tobacco, Planta 231 (2010) 1061–1076.
[19] J.P. Sanchez, N.H. Chua, Arabidopsis PLC1 is required for secondary responses to abscisic acid signals, Plant Cell 13 (2001) 1143–1154.
[20] P. Paul, S.K. Singh, B. Patra, X. Liu, S. Pattanaik, L. Yuan, Mutually regulated AP2/ERF gene clusters modulate biosynthesis of specialized metabolites in plants, Plant Physiol. 182 (2020) 840–856.
[21] S. Pattanaik, C.H. Xie, L. Yuan, The interaction domains of the plant Myc-like bHLH transcription factors can regulate the transactivation strength, Planta 227 (2008) 707–715.
[22] K.D. Edwards, N. Fernandez-Pozo, K. Drake-Stowe, M. Humphry, A.D. Evans, A. Bombarely, F. Allen, R. Hurst, B. White, S.P. Kernodle, A reference genome for Nicotiana tabacum enables map-based cloning of homeologous loci implicated in nitrogen utilization efficiency, BMC Genomics 18 (2017) 448.
[23] X. Hou, S.K. Singh, J.R. Werkman, Y. Liu, Q. Yuan, X. Wu, B. Patra, X. Sui, R. Lyu, B. Wang, X. Liu, Y. Li, W. Ma, S. Pattanaik, L. Yuan, Partial desensitization of MYC2 transcription factor alters the interaction with jasmonate signaling components and affects specialized metabolism, Int. J. Biol. Macromol. 252 (2023) 126472.
[24] X. Sui, S.K. Singh, B. Patra, C. Schluttenhofer, W. Guo, S. Pattanaik, L. Yuan, Cross-family transcription factor interaction between MYC2 and GBFs modulates terpenoid indole alkaloid biosynthesis, J. Exp. Bot. 69 (2018) 4267–4281.
[25] W.B. Langdon, Performance of genetic programming optimised Bowtie2 on genome comparison and analytic testing (GCAT) benchmarks, Biodata Min. 8 (2015) 1.
[26] N. Fernandez-Pozo, N. Menda, J.D. Edwards, S. Saha, I.Y. Tecle, S.R. Strickler, A. Bombarely, T. Fisher-York, A. Pujar, H. Foerster, The sol genomics network (SGN)—from genotype to phenotype to breeding, Nucleic Acids Res. 43 (2015) D1036–D1041.
[27] T. Shoji, M. Kajikawa, T. Hashimoto, Clustered transcription factor genes regulate nicotine biosynthesis in tobacco, Plant Cell 22 (2010) 3390–3409.
[28] H. Chen, Y. Zou, Y. Shang, H. Lin, Y. Wang, R. Cai, X. Tang, J.M. Zhou, Firefly luciferase complementation imaging assay for protein-protein interactions in plants, Plant Physiol. 146 (2008) 368.
[29] B. Cai, H. Ji, F.F. Fannin, L.P. Bush, Contribution of nicotine and nornicotine toward the production of N′-Nitrosonornicotine in air-cured tobacco *Nicotiana tabacum*, J. Nat. Prod. 79 (2016) 754–759.
[30] J.L. Qiu, L. Zhou, B.W. Yun, H.B. Nielsen, B.K. Fiil, K. Petersen, J. MacKinlay, G.J. Loake, J. Mundy, P.C. Morris, Arabidopsis mitogen-activated protein kinase kinases MKK1 and MKK2 have overlapping functions in defense signaling mediated by MEKK1, MPK4, and MKS1, Plant Physiol. 148 (2008) 212–222.
[31] S. Hayashi, M. Watanabe, M. Kobayashi, T. Tohge, T. Hashimoto, T. Shoji, Genetic manipulation of transcriptional regulators alters nicotine biosynthesis in tobacco, Plant Cell Physiol. 61 (2020) 1041–1053.
[32] Y. Liu, J. Shi, B. Patra, S.K. Singh, X. Wu, R. Lyu, X. Liu, Y. Li, Y. Wang, X. Zhou, Transcriptional reprogramming deploys a compartmentalized 'timebomb'in catharanthus roseus to fend off chewing herbivores, Plant Cell Environ. 48 (2025) 3236–3256.
[33] K. Gomi, D. Ogawa, S. Katou, H. Kamada, N. Nakajima, H. Saji, T. Soyano, M. Sasabe, Y. Machida, I. Mitsuhara, A mitogen-activated protein kinase NtMPK4 activated by SIPKK is required for jasmonic acid signaling and involved in ozone tolerance via stomatal movement in tobacco, Plant Cell Physiol. 46 (2005) 1902–1914.
[34] C. Xie, L. Yang, Y. Gai, MAPKKKs in plants: Multidimensional regulators of plant growth and stress responses, Int. J. Mol. Sci. 24 (2023) 4117.
[35] M.C. Suarez-Rodriguez, L. Adams-Phillips, Y. Liu, H. Wang, S.H. Su, P.J. Jester, S. Zhang, A.F. Bent, P.J. Krysan, MEKK1 is required for flg22-induced MPK4 activation in Arabidopsis plants, Plant Physiol. 143 (2007) 661–669.
[36] M. Gao, J. Liu, D. Bi, Z. Zhang, F. Cheng, S. Chen, Y. Zhang, MEKK1, MKK1/MKK2 and MPK4 function together in a mitogen-activated protein kinase cascade to regulate innate immunity in plants, Cell Res. 18 (2008) 1190–1198.
[37] T. Asai, G. Tena, J. Plotnikova, M.R. Willmann, W.L. Chiu, L. Gomez-Gomez, T. Boller, F.M. Ausubel, J. Sheen, MAP kinase signalling cascade in Arabidopsis innate immunity, Nature 415 (2002) 977–983.
[38] X. Sui, X. He, Z. Song, Y. Gao, L. Zhao, F. Jiao, G. Kong, Y. Li, S. Han, B. Wang, The gene NtMYC2a acts as a 'master switch'in the regulation of JA-induced nicotine accumulation in tobacco, Plant Biol. 23 (2021) 317–326.
[39] A. Movahedi, D. Hwarari, R. Dzinyela, S. Ni, L. Yang, A close-up of regulatory networks and signaling pathways of MKK5 in biotic and abiotic stresses, Crit. Rev. Biotechnol. 45 (2025) 473–490.
[40] D. Ren, Y. Liu, K.Y. Yang, L. Han, G. Mao, J. Glazebrook, S. Zhang, A fungal-responsive MAPK cascade regulates phytoalexin biosynthesis in Arabidopsis, Proc. Natl. Acad. Sci. U. S. A. 105 (2008) 5638–5643.
[41] T. Furuya, D. Matsuoka, T. Nanmori, Phosphorylation of *Arabidopsis thaliana* MEKK1 via Ca^{2+} signaling as a part of the cold stress response, J. Plant Res. 126 (2013) 833–840.
[42] D. Matsuoka, T. Furuya, T. Iwasaki, T. Nanmori, Identification of tyrosine autophosphorylation sites of Arabidopsis MEKK 1 and their involvement in the regulation of kinase activity, FEBS Lett. 592 (2018) 3327–3334.

Nicotine and Tobacco Research, 2026, **00**, 1–9
https://doi.org/10.1093/ntr/ntaf235
Advance access publication date 21 January 2026
Original Investigation

Comparison of the 1C2 Reference Filtered Cigar to the 1R6F Reference Filtered Cigarette

Amrita Machwe, PhD[1,2], Samuel B. Clark, BS[1], Halle Harned, BS[1], Tanvi Sawardekar, BS[1], Stacey A. Slone, MS[3], Huihua Ji, MS[4], David K. Orren, PhD[1,2]

[1]Department of Toxicology and Cancer Biology, 1056 V.A. Drive, University of Kentucky College of Medicine, Lexington, KY 40536, United States
[2]Markey Cancer Center, 800 Rose Street, University of Kentucky, Lexington, KY, 40536, United States
[3]Dr. Bing Zhang Department of Statistics, 302A Multidisciplinary Science Building, 725 Rose Street, University of Kentucky College of Arts and Sciences, Lexington, KY, 40536, United States
[4]Kentucky Tobacco Research and Development Center, 1401 University Drive, University of Kentucky College of Agriculture, Lexington, KY, 40546, United States

Corresponding Author: David K. Orren, PhD, *Department of Toxicology and Cancer Biology, University of Kentucky College of Medicine, 356 Bosomworth Health Sciences Research Building, 1095 V.A. Drive, Lexington, KY 40536-0305, United States. Telephone: 859-323-3612; E-mail: dkorre2@uky.edu*

Abstract

Introduction: Filtered cigars are a class of tobacco products that can be consumed similarly as conventional cigarettes. Here we have compared tobacco smoke condensates prepared from the 1C2 reference filtered cigar with those from the 1R6F reference cigarette with respect to effects on cell proliferation and viability and AhR-mediated gene expression.
Methods: Tobacco smoke condensates were prepared using ISO, Health Canada Intense (HCI) or Cigar Smoking (CSR) regimens and certain HPHCs were measured. Cell proliferation and viability assays were performed on immortalized human bronchial or oral epithelial cell lines. AHR-mediated gene expression was measured using a mouse hepatoma cell line engineered to express luciferase under control of the AHR promoter.
Results: Comparison of different smoking regimens found that the HCI regimen produces higher TPM levels, and higher AhR-mediated gene expression and toxicity when normalized to filler weight. Condensates from 1C2 reference filtered cigars resulted in higher AhR-mediated gene expression and reduced cell viability when compared with condensates prepared under the same conditions from the 1R6F reference cigarettes, again when normalized to filler weight.
Conclusions: Our results indicate that this reference filtered cigar is somewhat more toxic than the reference cigarette with the HCI regimen being most toxic. Our findings also suggest that some commercial filtered cigars may have at least as strong toxic effects as conventional cigarettes.
Implications: This study indicates that, if compared by filler weight, the 1C2 reference filtered cigar is more toxic than the 1R6F reference cigarette. Since these products were manufactured based on commercial products and at least some consumers of filtered cigars inhale smoke from these products into the lung, this suggests that some filtered cigars will be at least as harmful to consumers as conventional cigarettes.

Introduction

Filtered cigars are similar in appearance to cigarettes, except for the wrappers which are produced from tobacco leaf instead of paper. Their weight is somewhat heavier (100–200 mg) than a cigarette, which frees them from certain federal regulations; this includes filtered cigars being taxed like large cigars by federal law, at lower rates than for cigarettes.[1,2] Filtered cigars have evolved to be heavier than little/small cigars due to imposition of taxes on little/small cigars levied in 2009.[3,4] More importantly, little and filtered cigars are often consumed like cigarettes with inhalation into the lung, in contrast with large cigars and cigarillos. Approximately a third to a half of consumers of little or filtered cigars do not recognize that they are smoking a different product than conventional cigarettes.[5] The results of the 2012 National Survey on Drug Abuse and Health indicated that, in the US, an estimated million presumed cigarette users were actually smoking filtered cigars.[6] Currently in the US, filtered cigars are regulated now by the Food and Drug Administration (FDA) under the Family Smoking Prevention and Tobacco Control Act. In 2019, the FDA raised the age minimum to 21 to legally purchase tobacco products including filtered cigars. However, filtered cigars are not taxed like cigarettes and therefore less expensive, which has somewhat contributed to filtered cigar consumption. Compared to research done on reference and commercial cigarettes, filtered cigars have not been extensively studied.

Here, we compare 1C2 reference filtered cigars with the latest generation reference cigarette 1R6F as to certain chemical parameters and toxicology on immortalized cells. Notably, these reference products are manufactured by tobacco companies to reflect typical commercial cigarettes or filtered cigars, excluding any flavoring additives. We generated particulate phase condensates from each product and analyzed them for certain hazardous and potentially hazardous constituents (HPHCs) and used these condensates to treat cultured cells.

Received: July 1, 2025. **Revised:** September 19, 2025. **Accepted:** November 7, 2025

In some experiments, we compared different smoking regimens on our chemical and toxicology endpoints. Toxicological studies involved cell proliferation and viability experiments in immortalized human lung and oral epithelial cells, and induction of arylhydrocarbon receptor (AhR)-mediated gene expression. Importantly, AhR is a transcription factor known to respond to many exogenous chemicals including dioxin and polyaromatic hydrocarbons (PAHs) and induce transcription of genes involved in metabolism and immune signaling.[7] AhR pathway induction increases oxidative stress and potentiates activation of PAHs to intermediates that react with DNA.[8] AhR activation is thought to contribute to the toxicity of tobacco smoke. Our results indicate that reference filtered cigars are more toxic than reference cigarettes.

Methods

Tobacco Products and Generation of Tobacco Smoke and Smoke Condensates

1R6F reference cigarettes and 1C2 reference filtered cigars were obtained at the Center for Tobacco Research Products in the University of Kentucky College of Agriculture. All tobacco products were stored at -20°C until use. Reference cigarettes or filtered cigars were conditioned for 48 or 72 h at 22°C and 60% relative humidity according to ISO 3402:1999 and CORESTA Recommend Method (CRM 46), respectively. Tobacco smoke was generated from cigarettes or filtered cigars using a Cerulean linear smoking machine SM450 following ISO Non-intense smoking regimen 3308:2012 (ISO), Health Canada Intense (HCI) regimen, or CRM64 for Cigar Smoking Regimen (CSR). Total particulate matter (TPM) from cigarette- or filtered cigar-generated tobacco smoke was collected on 44 mm Cambridge filter pads. These filter pads were extracted with dimethyl sulfoxide (DMSO) and vacuum filtered using Whatman #1 filter paper to remove pad fiber to yield tobacco smoke condensates.

Chemical Analysis

DMSO condensates were diluted by methyl tert-butyl ether for alkaloid (nicotine and nornicotine) analysis or methanol for tobacco-specific nitrosamines (TSNAs) and PAH benzo[α}pyrene (B[α]P) analysis. TSNAs analyzed were 4-(methylnitrosamino)-1-(3-pyridyl)-1-butanone (NNK) and N′-nitrosonornicotine (NNN), N′-nitrosoanatabine (NAT), and N′-nitrosoanabasine (NAB). Alkaloid, TSNA, and B[α]P analysis were following modified CRM 62, CRM 75, and CRM58 protocols, respectively. Alkaloid analyses were done using a PerkinElmer Auto System XL gas chromatography (GC) with flame ionization detector. A Zebron capillary GC ZB-5 column (30 m × 0.53 mm, 1.50 μm film thickness from Phenomenex Inc.) was used for alkaloid determination. TSNA analyses were measured using an ACQUITY UPLC™ H-Class system connected to a Xevo TQD triple quadrupole mass spectrometry (Waters Corporation, Milford, MA, USA). Sample separation was achieved using a Waters ACQUITY UPLC™ XBridge BEH C18 2.1 × 50 mm column with 1.7 μm particles. B[α]P analysis was done using an Agilent 7890B GC system (Santa Clara, CA) coupled with an Agilent 7000C Triple Quad mass spectrometer. Chromatography was performed on a DB-17 GC capillary column (0.25 μm film, 0.25 mm × 30 m, Agilent Technologies).

Cell Culture

Immortalized human oral (OKF4) or bronchial (HBEC14) epithelial cells were maintained in keratinocyte serum-free media (GIBCO/Life Technologies) supplemented with recombinant human epidermal growth factor (0.5 ng/ml) and bovine pituitary extract (25 or 30 μg/ml, respectively); OKF4 media was also supplemented with 0.4 mM $CaCl_2$. Vessels used for OKF4 and HBEC14 experiments were precoated with fibronectin coating mix (Athena Enzyme Systems) to facilitate adherence. Mouse hepatoma cells containing AhR reporter gene, obtained from Michael Denison, were maintained in α-Minimal Essential Media supplemented with 10% fetal bovine serum and 1:100 dilution of antibiotic solution. Cells were maintained in a humidified atmosphere containing 20% oxygen and 5% CO_2.

Cell Proliferation and Viability Assays

OKF4 or HBEC14 cells were seeded into 6 well plates at 150 000 cells/well and allowed ∼48 h to resume proliferation. Cells were then treated (in triplicate) with indicated concentrations of condensates (or DMSO as vehicle control) in 2 ml fresh media. After 72 h, cells were washed with phosphate-buffered saline then released using 0.5 ml Trypsin–EDTA (0.05% for OKF4, 0.25% for HBEC14). A hematocytometer was used to count cell density of resulting cell suspensions without or with an equal volume of Trypan Blue, the latter to confirm viability of remaining attached cells. For each treated well (and for 4–6 untreated wells counted at the treatment time), total cell number was determined. Cell numbers of vehicle or condensate-treated wells were divided by cell number of vehicle-treated controls to yield percent survival. Relative cell numbers for each smoking regimen were statistically compared using a general linear model with percent concentration and smoking method with an interaction term. In experiments based on equivalent filler weight, since HCI was treated with lower dose range due to higher toxicity, the general quadratic model which considered dose as a continuous measure was fit to test changes in percent of total cells.

AHR Gene Reporter Assays

Mouse hepatoma cells (CALUX) are genetically engineered to stably harbor luciferase reporter gene under control of AhR promoter.[9] AhR pathway upregulates transcription of its target genes in response to numerous xenobiotic chemicals including certain tobacco constituents.[10] Thus, luciferase expression in this reporter assay reflects AhR upregulation by the test agent. Briefly, CALUX cells (20 000 cells/well) were seeded into 96 well luminescence-compatible microtiter plates and incubated for ∼24 h to permit attachment. Then, wells were treated (in triplicate at least) with indicated concentrations of cigarette or filtered cigar condensates; in parallel, 5–6 wells were treated with DMSO as vehicle controls. After 24 h, luciferase activity was assessed using the Steady-Luc Firefly Luciferase Assay Kit (Biotium) according to the manufacturer's instructions. Luminescence for each well was divided by mean luminescence of DMSO control wells to yield fold increase in luciferase reporter gene expression. Two-way ANOVAS were fit to assess differences across concentrations. For those outcomes in which smoking regime was also considered, three-way ANOVAs were fit to the log-transformed data to control for heteroscedacity. Statistical significance was determined by ad hoc pairwise tests. No adjustment was made

Table 1. Physical Properties of 1R6F and 1C2

Product	Regimen	Weight[2]	Ventilation	TPM (mg/rod)	TPM (mg/g filler weight)
1R6F	ISO	0.625	38.5	10.00	16.00
1R6F	ISO	0.625	38.5	10.50	16.80
1C2	ISO	1.039	23.7 ± 3.8	28. 71	30.16
1C2	ISO	1.039	23.7 ± 3.8	30.88	32.44
1R6F	CSR	0.625	38.5 ± 2.2	7.96	12.74
1C2	CSR	1.039	23.7 ± 3.8	22.06	23.17
1R6F	HCI	0.625	38.5 ± 2.2*	45.43	72.69
1C2	HCI	1.039	23.7 ± 3.8*	71.83	75.46

for multiple comparisons. Statistical analyses were completed using SAS 9.4 (SAS Institute Inc., Cary, NC, USA).

Results

Cigarette and Filtered Cigar Smoke Chemistry

1C2 reference filtered cigars and 1R6F reference cigarettes were smoked using ISO, CSR, or HCI regimen and condensates were collected on Cambridge filter pads; smoking regimens are described in Supplemental Table 1. Both ISO and CSR regimens generated comparable TPM levels/rod (Table 1). The HCI regimen generated considerably higher TPM levels/rod than other regimens (Table 1). Ventilation holes are covered during the HCI smoking regimen, resulting in lower temperature burning of tobacco and higher TPM levels. When using the HCI method, TPM/rod levels were ~4.5-fold higher than ISO method with 1R6F reference cigarette, and ~2.5 fold higher with 1C2 reference filtered cigar. When using ISO or CSR regimen, TPM levels based on equivalent filler weight were 1.91 or 1.82 times higher, respectively, for filtered cigar compared to cigarette condensates. This suggests the reference filtered cigar might be more toxic than the reference cigarette. However, when HCI regimen is utilized, the TPM levels for the filtered cigar and cigarette based on equivalent filler weight were approximately equal. Thus, both filtered cigar and cigarette clearly produced higher TPM levels and were likely more toxic using the HCI regimen, but blockage of ventilation with this method made them have nearly equivalent TPM levels to each other by filler weight.

Smoke condensates produced by different regimens were subsequently compared for analysis of nicotine, TSNAs and B[α]P present. The amounts of condensate used here and below were normalized to filler weight, to best account for different filtered cigar and cigarette styles and weights. When normalized to equivalent filler weight, nicotine delivered in tobacco smoke condensate was only slightly greater when using ISO or CSR regimen for 1C2 than 1R6F, but when HCI regimen was used, nicotine levels were much higher for both products and were significantly higher in 1R6F than 1C2 (Figure 1A). This suggests the design of both products favors delivery of nicotine because that is the purpose of smoking, particularly under HCI conditions where ventilation is lower. Different patterns emerge when considering levels of nornicotine, TSNAs and B[α]P between 1C2 and 1R6F with various smoking regimens. For all these HPHCs, levels in tobacco smoke condensate were higher using the HCI regimen than the other two regimens (Figure 1B–G); this fits with TPM levels of these condensates. More importantly, when comparing same regimens used between the two tobacco products, levels of these toxic compounds (except NAT) were substantially higher (~1.8 to >3 fold, depending on regimen and specific compound) in 1C2 reference filtered cigar than 1R6F reference cigarette (Figure 1B–F). This list of compounds higher in the reference filtered cigar includes nornicotine, B[α]P, and TSNAs NNN, NNK, and NAB. NAT levels were more comparable between the two products using ISO and CSR regimens and somewhat higher in 1R6F than 1C2 using HCI regimen (Figure 1G). As this filtered cigar was based on a specific commercial product, this suggests some filtered cigars would be considerably more toxic on a filler weight basis than cigarettes. Of course, this needs to be demonstrated with commercial filtered cigars, some of which may have lower HPHC levels than 1C2 reference filtered cigar. In fact, a recent survey of filtered cigars showed that most had much higher levels of NNN and NNK in their tobacco smoke than a reference cigarette.[11]

Effects of Reference Filtered Cigar and Cigarette Condensates on Cell Proliferation and Viability

To determine effects of our condensates on proliferation and viability, cells were counted after 72 h of treatment. Initially, we titrated TPM levels to determine the best range of concentration to compare cytotoxicities from 1C2 and 1R6F condensates. For these comparisons, we used a single treatment of condensate on OKF4 or HBEC14 cell lines, which were chosen for study because they represent immortalized normal oral and bronchial epithelial cells, respectively. Notably, each cigarette or filtered cigar condensate showed similar effects on both cell lines. At <20 μg TPM/ml of media, effects on both HBEC14 proliferation and viability were negligible. At 20-120 μg TPM/ml media, we observe marked effects on cell proliferation and viability, so we focused our assays in this concentration range. When HBEC14 cells were treated with 1R6F or 1C2 condensates prepared by ISO regimen, we observed little or no difference in cytotoxicity when condensate concentrations were normalized to equivalent μg TPM/ml media (Figure 2A). However, 1R6F showed statistically significant less toxicity at 100 μg TPM/ml media dose. We observed similar results when OKF4 cells were treated with these ISO condensates, again with statistical significance at the highest dose tested (Figure 2B). Further, there was no significant difference at any dose when OKF4 cells were treated with 1C2 or 1R6F condensates prepared using HCI regimen (Figure 2C); this agrees with these condensates showing similar μg TPM/ml DMSO (Table 1). This suggests that reference cigarette and reference filtered cigar have nearly equivalent cytotoxicity when based on equivalent TPM levels. This result implies that, when compared based on equivalent

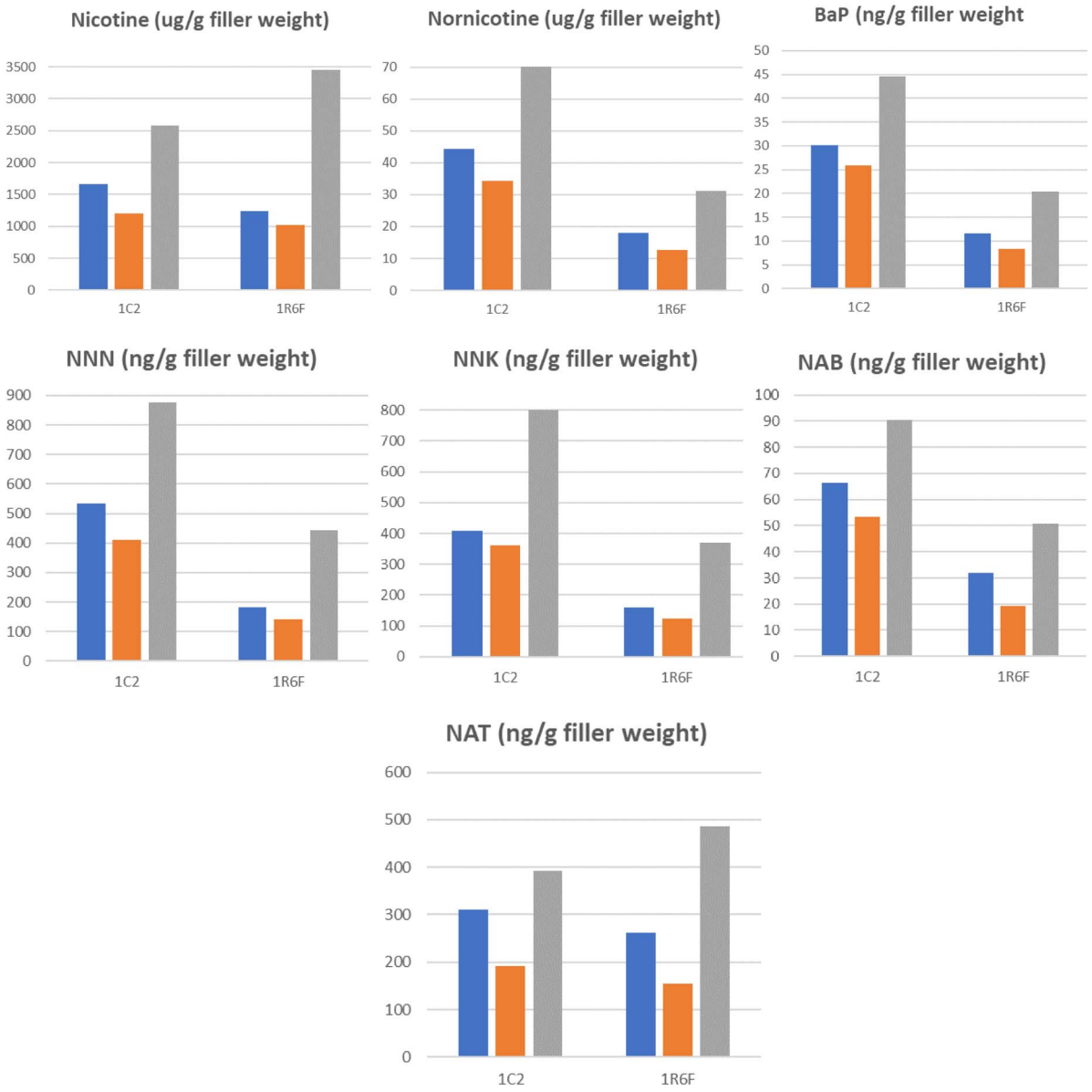

Figure 1. Concentrations of certain HPHCs in 1C2 reference filtered cigar and 1R6F reference cigarette smoke condensates. Concentrations of individual HPHCs based on filler weight in the particulate phase smoke condensates prepared from the 1C2 reference filtered cigar (*left in each panel*) and the 1R6F reference cigarette (*right in each panel*) are depicted in the bar graphs under ISO (*blue*), CSR (*orange*), and HCI (*gray*) smoking regimens.

TPM, 1C2 filtered cigar and 1R6F cigarette had roughly equal levels of toxic compounds. We then compared the different regimens as to their effects on cell proliferation and viability. When OKF4 cells were treated with 1C2 condensate concentrations normalized to μg TPM/ml media, we did not observe significantly different effects on cytotoxicity between ISO and CSR regimens although there was a trend for CSR to be slightly less toxic (Figure 3A). Notably, HCI regimen was less toxic at almost all concentrations tested when normalizing to TPM. These results were statistically significant for every dose when CSR and HCI regimens were compared, and for 20, 60, and 100 μg TPM/ml doses when ISO and HCI regimens were compared. In fact, at 100 μg TPM/ml media, some 16.5% of OKF4 cells survived HCI condensate treatment while ISO and CSR regimens were nearly completely cytotoxic. The same experiment was done with HBEC14 cells with slightly different results. HBEC14 cells survived the highest dose (100 μg TPM/ml media) of 1C2 HCI condensate while those treated with ISO or CSR condensate did not (Figure 3B); this result was statically significant when either CSR or ISO regimen was compared to HCI regimen. However, at lower doses, no clear difference existed between condensates prepared by different regimens.

We performed additional experiments in which 1C2 and 1R6F condensates were normalized to tobacco filler weight instead of TPM to better give a understanding of the toxicity of filtered cigars compared with cigarettes. Filler weights for the 1C2 and 1R6F are given in Table 1. After 72 h of treatment with concentrations of condensate varying from 0.35-6 μg filler weight/ml media, we counted HBEC14 cells remaining. When using ISO regimen and normalizing to filler weight, 1C2 cytotoxicity was significantly greater than 1R6F (Figure 4A). This result suggests that, if compared by filler weight, this filtered cigar is more toxic than reference cigarettes. When comparing smoking regimens to each other and normalizing to filler weight, 1C2 cytotoxicities with different regimens

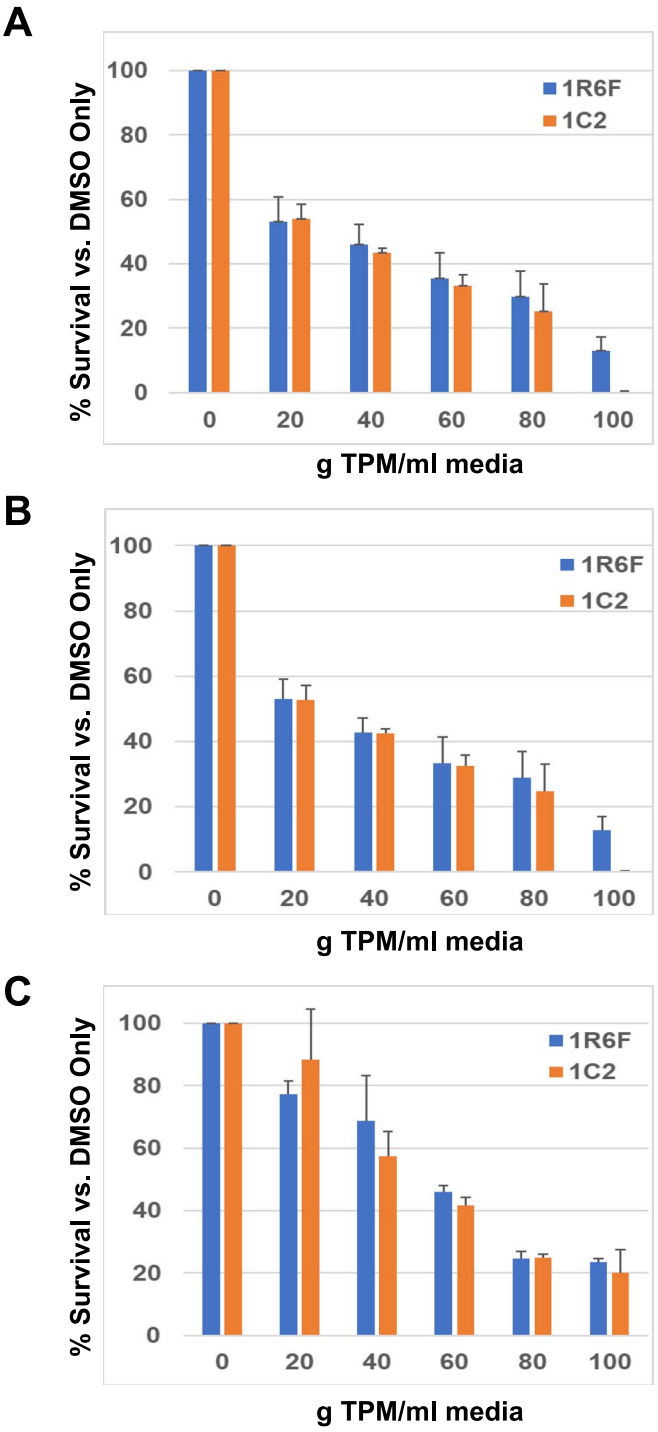

Figure 2. Survival of HBEC14 and OKF4 cells after treatment with 1C2 and 1R6F condensates prepared by the ISO regimen, normalizing to TPM. (A) OKF4 and (B) HBEC14 cells were seeded in 6 well plates in triplicate at 75 000 cells/well then after 72 h treated with either 1R6F reference cigarette (*blue bars*) or 1C2 reference filtered cigar (*orange bars*) smoke condensate prepared using the ISO regimen from 0 to 100 μg TPM/ml media. (C) OKF4 cells were treated from 0 to 100 μg TPM/ml media with 1R6F (*blue bars*) or 1C2 (*orange bars*) condensates prepared by the HCI regimen. Cells were counted after another 72 h, normalized to the untreated (DMSO only) control and the means and standard errors plotted. * = statistically significant difference, p = .0418 and .0327 for panels A and B, respectively.

were much different from each other (Figure 4B). HCI condensate had the largest cytotoxic effect, with near complete loss of viability at 1.9 μg filler weight/ml media. ISO regimen showed lower cytotoxicity over the entire concentration range tested than HCI regimen and did not reach complete cytotoxicity until 3.5 μg filler weight/ml media. CSR regimen showed the lowest effect on cell viability, with consistently lower toxicity than HCI and ISO regimens over 1.4–3.5 μg filler weight/ml media and with ~18% of cells remaining viable at the 3.5 μg filler weight/ml media concentration. This indicates that, when compared based on equivalent filler weight, the regimen used to smoke filtered cigars has a large effect on cell viability and suggests that concentrations of compounds produced by smoking the same filtered cigars under different

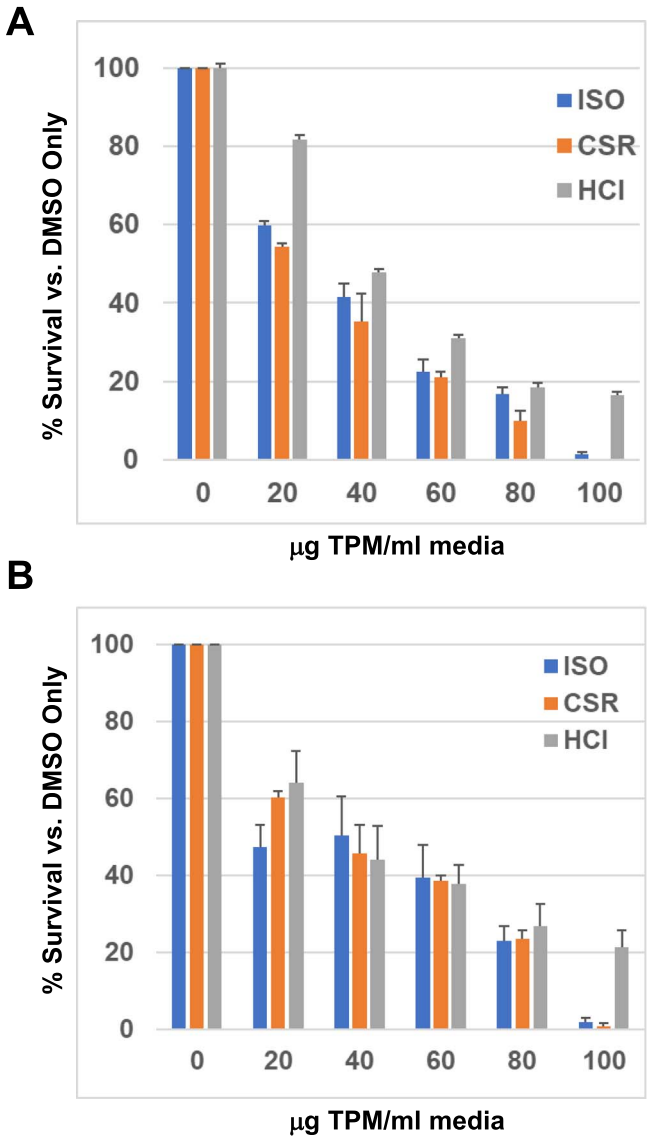

Figure 3. Survival of HBEC14 and OKF4 cells after treatment with 1C2 condensates prepared by the ISO, CSR, and HCI regimens, normalized to TPM. (A) OKF4 or (B) HBEC14 cells were seeded in 6-well plates in triplicate at 75 000 cells/well. After 72 h, the cells were treated with 0-100 μg TPM/ml media with 1C2 reference filtered cigar smoke condensate prepared using the ISO (*blue bars*), CSR (*orange bars*), or HCI (*gray bars*). Regimens. Cells were counted after another 72 h, normalized to the untreated (DMSO only) control and the means and standard errors plotted. For panel a, statistically significant differences were observed were observed between CSR and HCI regimens at all doses and ISO and HCI regimens at 20, 60, and 100 μg TPM/ml media doses. For panel B, statistically significant differences were only observed between the CSR and HCI regimens and the ISO and HCI regimens at 20 and 100 μg/ml TPM/ml media.

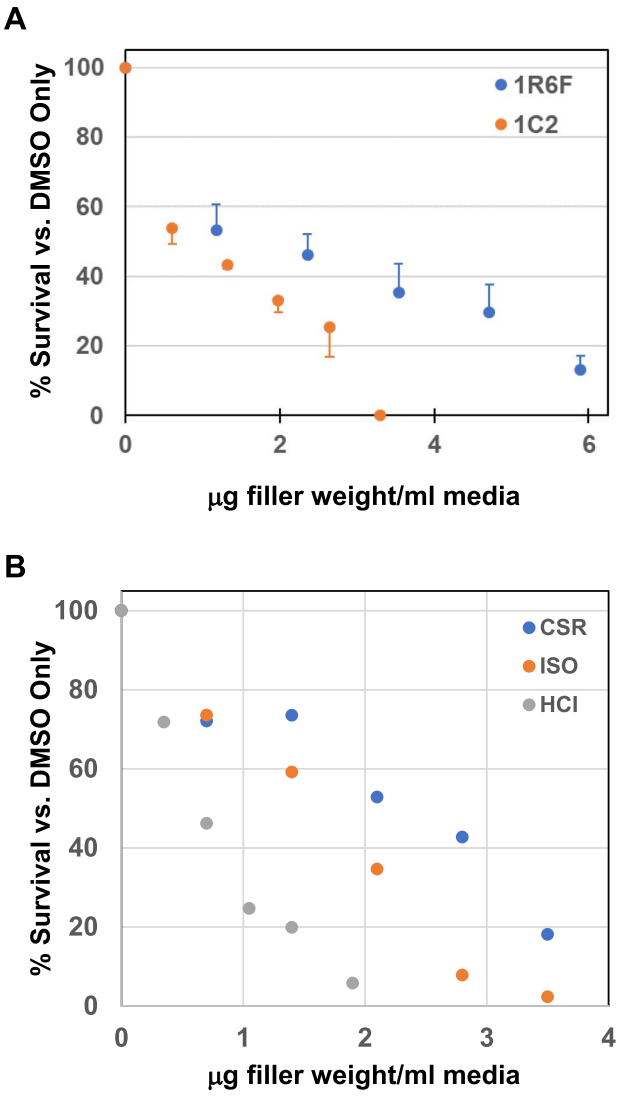

Figure 4. Survival of HBEC14 cells after treatment with 1C2 condensates prepared by the ISO, CSR, and HCI regimens, based on filler weight. HBEC14 cells were seeded in 6-well plates in triplicate at 75 000 cells/well. (A) after 72 h, the cells were treated with the indicated concentrations (normalized to filler weight for each product) of 1R6F (*blue dots*) or 1C2 (*orange dots*) prepared by the ISO smoking regimen. Cells were counted after another 72 h, normalized to the untreated (DMSO only) control and the means and standard errors plotted. (B) after 72 h, the cells were treated with 0, 0.35, 0.7, 1.05, 1.4, 1.9, 2.1, 2.8, or 3.5 μg filler weight/ml media with 1C2 reference filtered cigar smoke condensate prepared using the ISO (*blue dots*), CSR (*orange dots*), or HCI (*gray dots*). Cells were counted and normalized as above and the means plotted. *p* values were statistically significant for comparisons between the ISO and HCI regimens and the CSR and HCI regimens ($p < .0001$ for both comparisons at the 0.7 and 1.4 μg filler weight/ml).

regimens are different and impact HBEC cells differently. This can be readily seen in our limited chemical analysis of condensates prepared under the different regimens; levels of nicotine, nornicotine, all of the TSNAs are ~1.4-2-fold higher when 1C2 filtered cigar is smoked using HCI compared to either ISO or CSR regimen (Figure 1). In fact, the relative cytotoxicity of each 1C2 condensate follows these HPHC amounts produced under different regimens, ie the cytotoxicity of CSR < ISO < HCI.

Effects of Cigarettes Versus Filtered Cigars on AhR Gene Induction

The AhR pathway responds to xenobiotic compounds to induce genes that metabolize and theoretically help detoxify these compounds.[7] Several compounds in tobacco smoke are known to induce AhR-mediated gene expression, particularly PAHs such as B[α]P.[10] AhR upregulates CYP1A1 and CYP1B1 that metabolize PAHs to intermediates that damage DNA.[12] We used mouse hepatoma (CALUX) cells with an AhR reporter system—ie engineered to express luciferase under

control of AhR promoter.[9] First, we used ISO-generated condensates normalized to equivalent TPM levels to titrate the AhR response. Notably, AhR gene induction (above background signal mediated by DMSO) by 1C2 reference filtered cigar condensate was detectable at 1.496-1.584-fold at 0.01 μg TPM/ml media while a barely detectable response (1.123–1.251 fold) was observed with 1R6F reference cigarette condensate at the same concentration (Supplemental Table 2). When CALUX cells were treated with higher condensate concentrations, we observed a dose-dependent response as expected. Filtered cigars gave a somewhat stronger response at every concentration up to 5 μg TPM/ml media, although this effect was small (Supplemental Figure 1). Stronger responses of 1C2 filtered cigar compared to 1R6F cigarette were observed in repeated experiments with multiple condensates tested. These results strongly suggest that chemical content of reference filtered cigar condensates (prepared using ISO regime) had higher levels of compounds that induce the AhR response than reference cigarettes.

Next, 1R6F and 1C2 condensates using ISO, HCI, and CSR smoking regimens were compared for the ability to induce the AhR response, first normalizing to equivalent TPM. When measured over a concentration range from 0.1 to 10 μg TPM/ml media, each condensate induced dose-dependent AhR responses. ISO and CSR condensates from 1R6F cigarette and 1C2 filtered cigar gave similar results (Figure 5A), although 1C2 showed slightly stronger responses than 1R6F condensate at the lowest concentrations (0.1–1 μg TPM/ml media). 1R6F HCI condensate showed lower induction of AhR response at each respective concentration than ISO and CSR condensates. This agrees with results showing lower cytotoxicity of 1R6F HCI than ISO and CSR condensates when compared based on equivalent TPM. 1C2 HCI condensates showed similar AhR induction compared to 1C2 ISO and CSR condensates at concentrations ranging from 0.1 to 1 μg TPM/ml media, but somewhat higher induction at the highest concentrations (4 and 10 μg TPM/ml media). However, if you compare 1R6F and 1C2 HCI condensates to each other, 1C2 condensates showed stronger (statistically significant) induction of AhR response at each respective concentration. For comparing these ISO condensates, all doses were statistically significant except 4 μg TPM/ml media. CSR condensates were not significantly different (except 0.4 μg TPM/ml media). These results suggest that, even when you normalize to equivalent TPM, 1C2 condensates have higher concentration of compounds that mediate AhR induction.

We next compared AhR response of all 1C2 and 1R6F condensates, normalizing to filler weight. 1C2 filtered cigars have ~50% more tobacco (1.039 g/rod) than 1R6F reference cigarette (0.625 g/rod). In these experiments, concentrations tested ranged from 1 to 100 μg filler weight/ml media. Results of these experiments showed clearly that, for both 1R6F and 1C2, condensate prepared from HCI regimen induced AhR responses more strongly at each respective concentration than ISO and CSR condensates, which were very similar (Figure 5B). Importantly, 1C2 condensates induced AhR responses more strongly than 1R6F condensates prepared by the same regimen at each respective concentration (Figure 5B, *compare 1C2 titrations at right to 1R6F titrations at left*); this effect was highly statistically significant at each concentration ($p < .0001$). We also considered the possibility that smokers of these products might consume them based on the number of rods. When compared on a per rod basis, this simply recapitulated and increased differences seen when compared on basis of filler weight (Supplemental Figure 2). Within the same tobacco product category, HCI condensates more strongly induced AhR responses than ISO and CSR condensates. 1C2 condensates showed stronger responses than their respective 1R6F counterparts, and when smoked under HCI regimen tested at the three lowest concentrations showed the highest induction of AhR responses. The two highest concentrations

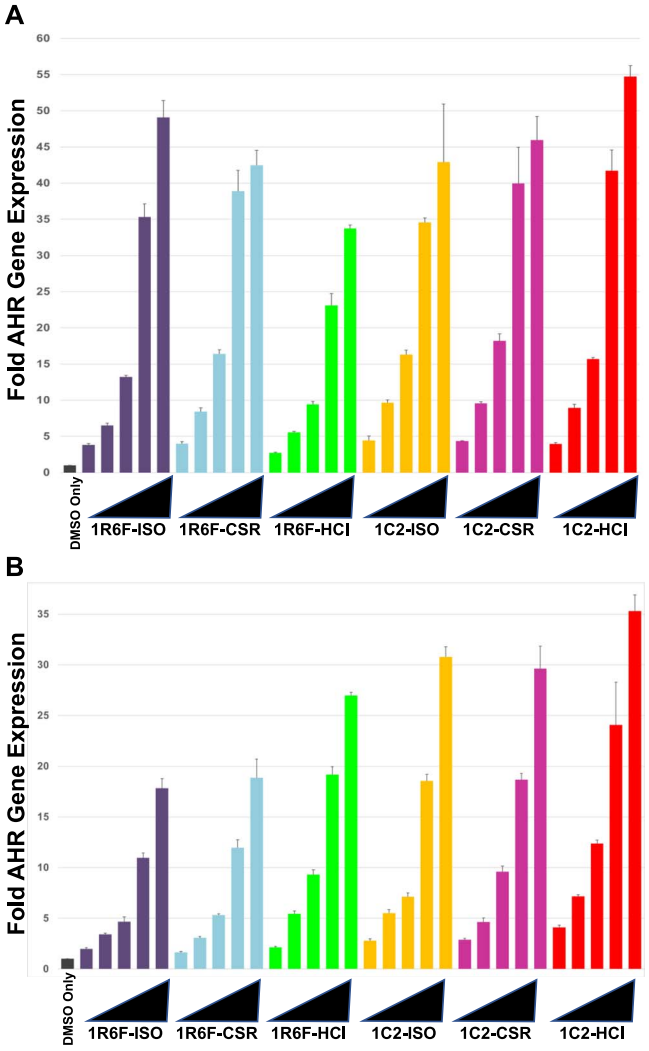

Figure 5. AHR reporter gene expression induced by 1R6F and 1C2 condensates prepared by the ISO, CSR, or HCI regimens. CALUX cells were seeded at 20000 cells/well in a microtiter plate. After 24 h, cells were treated in quadruplicate with 1R6F reference cigarette (*at left*) or 1C2 reference filtered cigar (*at right*) smoke condensate prepared by the ISO, CSR, or HCI regimen (A) normalized to equivalent TPM at 0.1, 0.4, 1.0, 4.0, and 10.0 μg TPM/ml media or (B) normalized to equivalent filler weight from 1.0, 4.0, 10, 40, and 100 μg filler weight/ml media; 6 wells were treated with DMSO only as vehicle controls. After another 24 h, luminescence generated by luciferase activity was measured using a microplate reader, readings were normalized to the mean for the vehicle (DMSO only) control, and means and standard errors were plotted. For panel a, *p* values for comparison between 1R6F and 1C2 are significant at all doses for the HCI regimen ($p < .0001$) and at the 0.4 dose for the CSR regimen ($p = .02$) and at 0.1, 0.4, 1, & 10 doses for the ISO regimen ($p < .01$). For panel B, *p* values for comparison between 1R6F and 1C2 are significant at all doses for the HCI, CSR, and ISO regimens ($p < .0001$).

had lower responses, presumably due to effects on cell proliferation and viability. These effects were all statistically significant when respective 1C2 condensate was compared with 1R6F condensate, except for 1:10000 HCI concentration and above which we believe caused cytostatic or cytotoxic effects and CSR regimen at 1:4000. From these results, condensates prepared using HCI regimen have higher concentrations of compounds that induce AhR responses than ISO and CSR regimens. Furthermore, 1C2 filtered cigar condensates induce AhR responses more strongly than 1R6F condensates when compared based on filler weight and the same regimen. So, 1C2 condensates should have higher concentrations of compounds that induce this response than 1R6F condensates, at least when smoked by the same regimen.

Discussion

Here, we have compared tobacco smoke condensates of 1C2 reference filtered cigar with 1R6F reference cigarette, prepared under different ISO, CSR, and HCI smoking regimens. It is quite clear that, when HCI smoking regimen is used, TPM yield is much higher. It is roughly 4.3-fold for reference cigarette and 2.4-fold for reference filtered cigar on a per rod basis and 4.4-fold for reference cigarette and 2.4-fold for reference filtered cigar when based on equivalent filler weight than when using ISO regimens. CSR regimen yielded slightly lower TPM levels than ISO regimen for both tobacco products, so HCI differences with CSR regimen are even greater. Based on filler weight, nicotine, nornicotine, most TSNAs and B[α]P are clearly higher when using HCI regimen, suggesting blocking ventilation holes creates higher delivery of these HPHCs into smoke and its particulate phase. When effects of condensates are compared based on equivalent TPM levels, this tends to even out differences between condensates when assessing cytotoxicity and AhR response. However, even when compared based on equivalent TPM levels for each regimen, 1C2 reference filtered cigar induces AhR responses more strongly than 1R6F reference cigarette. This certainly suggests compounds (likely HPHCs) produced from 1C2 that induce AhR responses are at somewhat higher levels and much higher levels than in 1R6F, when compared based on equivalent TPM levels and equvalent filler weights, respectively. Notably, B[α]P (and likely other PAHs), which are known to induce AhR responses, is substantially higher in reference filtered cigar than reference cigarette condensates and highest when HCI regimen is utilized.

We believe it is most accurate to compare tobacco products and smoking regimens based on normalization to filler weight. This takes into consideration differences between weights of products and allows direct comparison of regimens. When their effects were compared based on equivalent filler weight, 1C2 filtered cigar condensate was significantly more cytotoxic to HBEC14 cells than 1R6F reference cigarette, when both were prepared using ISO smoking regimen. Again, when compared based on filler weight, 1C2 condensates more strongly induced AhR-mediated gene expression than 1R6F condensates irrespective of regimen used. For 1C2 condensates when normalized to filler weight, HCI was clearly the most cytotoxic regimen while ISO regimen was slightly more toxic than CSR regimen. HCI regimen also induced stronger AhR responses than either ISO or CSR regimen; this was true for both 1C2 and 1R6F condensates. Taken together, these results suggest that burning of the same weight of tobacco in 1C2 filtered cigar produced higher levels of compounds that create cytotoxicity and induced AhR responses more strongly than 1R6F cigarette. HCI regimen produced much higher levels of these compounds than ISO or CSR regimens. This is borne out if one examines the limited number of compounds tested in these condensates. When compared based on filler weight, HCI regimen gives much higher levels of nicotine, nornicotine, most TSNAs and B[α]P than ISO or CSR regimens. Perhaps more importantly, 1C2 filtered cigar produces higher levels (~2-fold) of nornicotine, B[α]P and all TSNAs except NAT than 1R6F cigarette. Since 1C2 was produced based on commercial filtered cigar products, this indicates that at least some filtered cigars, if inhaled like cigarettes, would be more toxic than reference cigarettes. Of course, commercial filtered cigar products should be tested to determine their relative toxicity compared to this reference filtered cigar and reference and commercial cigarettes. Reportedly, the tobacco content of filtered cigars is much different with regard to blend, texture, and curing.[1] 1R6F cigarette also has higher overall ventilation than 1C2 filtered cigar (38.5 vs. 23.7, see Table 1). These factors could play roles in the higher yield of HPHCs and toxic effects of filtered cigars when compared based on filler weight.

One limitation of this study is it only compared reference filtered cigars to reference cigarettes, so more research needs to analyze HPHCs and biological effects of commercial filtered cigars. Nevertheless, our results suggest that some commercial filtered cigars may be at least as toxic or potentially more toxic than conventional cigarettes. Notably, the commercial filtered cigars are considered as cigars and not regulated like conventional cigarettes, so retail prices for these filtered cigar products tend to be lower, encouraging their consumption compared to cigarettes. However, these filtered cigars are often consumed like cigarettes, being inhaled into smokers' lungs. Many consumers of filtered cigars don't make the distinction between these products and conventional cigarettes.[5]

Author Contributions

Amrita Machwe (Conceptualization [equal], Formal Analysis [equal], Investigation [equal], Methodology [equal], Writing—original draft [equal]), Samuel B. Clark (Data curation [equal], Formal Analysis [equal], Investigation [equal], Methodology [equal]), Halle Harned (Data curation [equal], Formal Analysis [equal]), Tanvi Sawardekar (Data curation [equal], Formal Analysis [equal]), Stacey Slone (Formal Analysis [equal], Validation [equal]), Huihua Ji (Data curation [equal], Formal Analysis [equal], Investigation [equal], Methodology [equal], Resources [equal]), and David K. Orren (Conceptualization [equal], Formal Analysis [equal], Funding acquisition [lead], Investigation [equal], Project administration [lead], Supervision [lead], Validation [equal], Writing—original draft [equal])

Supplementary Material

Supplementary material is available at *Nicotine and Tobacco Research* online.

Funding

The authors would like to acknowledge the financial support from grant/contract #5UC2FD006890 from the United States Food and Drug Administration.

Declaration of Interest

The authors have no conflict of interest to declare.

Acknowledgments

The Orren lab would like to acknowledge the myriad contributions of the CTRP and the Kentucky Tobacco Research and Development Center of the University of Kentucky College of Agriculture. We would also like to acknowledge the financial support via grant/contract #5UC2FD006890 and other contributions (including critical reading by members) of the US Food and Drug Administration.

Data Availability

Data available on request.

References

1. Hamad SH, Johnson NM, Tefft ME, *et al.* Little cigars vs 3R4F cigarette: physical properties and HPHC yields. *Tob Regul Sci*. 2017;**3**(4):459-478.
2. Tax rates for tobacco products. ttb.gov/taxes/tax-audit/tax-and-fee-rates. Accessed September 9, 2025.
3. Delnevo CD, Hrywna M, Giovenco DP, Miller Lo EJ, O'Connor RJ. Close, but no cigar: certain cigars are pseudo-cigarettes designed to evade regulation. *Tob Control*. 2017;**26**(3):349-354.
4. Reilly SM, Goel R, Bitzer Z, *et al.* Little cigars, filtered cigars, and their carbonyl delivery relative to cigarettes. *Nico Tob Res*. 2018;**20**(suppl_1):S99-S106.
5. Caseus M, Garmon J, Hrywna M, Delnevo CD. Cigarette smokers' classification of tobacco products. *Tob Control*. 2016;**25**(6):628-630.
6. US Department of Health and Human Services. Substance abuse and mental health services administration. Center for Behavioral Health Statistics and Quality. In: *National Survey on Drug Use and Health*. Vol. **2012**. Ann Arbor, MI: Inter-university Consortium for Political and Social Research [distributor]; 2015:ICPSR34933-v3 10.3886/ICPSR34933.v3.
7. Kou Z, Dai W. Aryl hydrocarbon receptor: its roles in physiology. *Biochem Pharmacol*. 2021;**185**:114428.
8. Holme JA, Vondráček J, Machala M, *et al.* Lung cancer associated with combustion particles and fine particulate matter (PM2.5) —the roles of polycyclic aromatic hydrocarbons (PAHs) and the aryl hydrocarbon receptor (AhR). *Biochem Pharmacol*. 2023;**216**:115801.
9. Han D, Nagy SR, Denison MS. Comparison of recombinant cell bioassays for the detection of ah receptor agonists. *Biofactors*. 2004;**20**(1):11-22.
10. Kitamura M, Kasai A. Cigarette smoke as a trigger for the dioxin receptor-mediated signaling pathway. *Cancer Lett*. 2007;**252**(2):184-194.
11. Edwards SH, Hassink MD, Taylor KM, *et al.* Tobacco-specific nitrosamines in the tobacco and mainstream smoke of commercial little cigars. *Chem Res Toxicol*. 2021;**34**(4):1034-1045.
12. Moorthy B, Chu C, Carlin DJ. Polycyclic aromatic hydrocarbons: from metabolism to lung cancer. *Toxicol Sci*. 2015;**145**(1):5-15.

Nicotine and Tobacco Research, 2026, 00, 1–9
https://doi.org/10.1093/ntr/ntaf235
Original Investigation

FISCAL YEAR 2025 – 2026

FINANCIAL REPORT

January 1, 2026 – March 31, 2026

QUARTERLY REPORT

TOBACCO RESEARCH INCOME
INCOME COMPARISON

Fiscal Years	2020-2021	2021-2022	2022-2023	2023-2024	2024-2025	2025-2026
July	$ 136,565.92	$ 102,816.87	$ 113,853.04	$ -	$ 97,579.97	$ 84,421.42
August	$ 11,873.82	$ 148,863.59	$ 121,485.75	$ 235,814.07	$ 113,878.38	$ 94,787.78
September	$ 261,157.23	$ 138,395.19	$ 143,503.64	$ 116,834.55	$ 112,212.24	$ 109,920.98
1st QUARTER	**$ 409,596.97**	**$ 390,075.65**	**$ 378,842.43**	**$ 352,648.62**	**$ 323,670.59**	**$ 289,130.18**
October	$ 141,682.93	$ 138,913.78	$ 131,512.77	$ 84,290.07	$ 86,565.34	$ 96,740.93
November	$ 135,157.14	$ 101,844.54	$ 101,050.68	$ 132,736.05	$ 88,478.89	$ 104,074.91
December	$ 159,616.92	$ 138,232.14	$ 113,515.64	$ 81,648.61	$ 90,136.26	$ 97,484.98
2nd QUARTER	**$ 436,456.99**	**$ 378,990.46**	**$ 346,079.09**	**$ 298,674.73**	**$ 265,180.49**	$ 298,300.82
January	$ 93,056.96	$ 116,044.01	$ 111,657.62	$ 101,501.91	$ 78,472.89	$ 80,225.85
February	$ 125,797.09	$ 89,271.71	$ 78,955.86	$ 77,922.09	$ 125,701.11	$ 73,327.03
March	$ 143,903.75	$ 140,521.53	$ 119,175.49	$ 105,636.69	$ 45,037.80	$ 95,603.89
3rd QUARTER	**$ 362,757.80**	**$ 345,837.25**	**$ 309,788.97**	**$ 285,060.69**	**$ 249,211.80**	$ 249,156.77
April	$ 144,970.47	$ 127,449.97	$ 79,639.90	$ 119,161.48	$ 94,449.22	$ -
May	$ 100,238.76	$ 148,769.94	$ 120,890.24	$ 88,889.28	$ 80,887.20	$ -
June	$ 211,130.06	$ 121,204.33	$ 149,991.92	$ 154,407.96	$ 103,211.51	$ -
4th QUARTER	**$ 456,339.29**	**$ 397,424.24**	**$ 350,522.06**	**$ 362,458.72**	**$ 278,547.93**	$ -
TOTAL INCOME	**$ 1,665,151.05**	**$ 1,512,327.60**	**$ 1,385,232.55**	**$ 1,298,842.76**	**$ 1,116,610.81**	**$ 836,587.77**

FISCAL YEAR 2025-2026 INCOME AND FINANCIAL REPORT KTRDC 3rd QUARTER REPORT

Funds Center	Funds Center Name	Category	Original Budget	Annual Budget	Prior Month Balance	Current Month Actual	YTD Actual	YTD Encumbrances	Available Budget
1235410080	KTRDC HOLDING ACCOUNT	Revenue	($1,723,000.00)	($1,723,000.00)	($740,983.88)	($95,603.89)	(836.587.77)		($263,412.23)
1235410080	Result	Total	($1,723,000.00)	($1,723,000.00)	($740,983.88)	($95,603.89)	(836.587.77)		($263,412.23)
1235410090	KENTUCKY TOBACCO RESEARCH BOARD	Operating Expenses		$1,000.00					$1,000.00
1235410090	Result	Total		$1,000.00					$1,000.00
1235410100	KTRDC ADMINISTRATION	Salaries	$1,723,000.00	$260,000.00	$117,620.46	$10,809.76	$128,430.22	$35,481.36	$96,088.42
1235410100	KTRDC ADMINISTRATION	Benefits			$48,000.17	$4,059.90	$52,060.07	$12,529.72	($64,589.79)
1235410100	KTRDC ADMINISTRATION	Operating Expenses			$2,787.33	$4,452.31	$7,239.64	$0.00	($7,239.64)
1235410100	KTRDC ADMINISTRATION	Recharges			$28.00	$1.75	$29.75		($29.75)
1235410100	Result	Total	$1,723,000.00	$260,000.00	$168,435.96	$19,323.72	$187,759.68	$48,011.08	$24,229.24
1235410110	KTRDC PERSONNEL	Salaries			$259,946.55	$29,265.81	$289,212.36	$85,464.08	($374,676.44)
1235410110	KTRDC PERSONNEL	Benefits			$76,200.34	$9,306.10	$85,506.44	$27,557.81	($113,064.25)
1235410110	KTRDC PERSONNEL	Operating Expenses		$1,000,000.00	$10,036.82	($255.51)	$9,781.31		$990,218.69
1235410110	KTRDC PERSONNEL	Recharges			$31,266.92	$3,308.22	$34,575.14		($34,575.14)
1235410110	Result	Total		$1,000,000.00	$377,450.63	$41,624.62	$419,075.25	$113,021.89	$467,902.86
1235410120	KTRDC PUBLICATIONS AND TRAVEL	Operating Expenses		$25,000.00	$8,981.30		$8,981.30		$16,018.70
1235410120	KTRDC PUBLICATIONS AND TRAVEL	Recharges			$754.20		$754.20		($754.20)
1235410120	Result	Total		$25,000.00	$9,735.50		$9,735.50		$15,264.50
1235410130	KTRDC BUILDING MAINTENANCE	Operating Expenses		$50,000.00	$17,575.62	$1,666.68	$19,242.30	$0.00	$30,757.70
1235410130	KTRDC BUILDING MAINTENANCE	Recharges			$1,852.07	$1,449.40	$3,301.47		($3,301.47)
1235410130	Result	Total		$50,000.00	$19,427.69	$3,116.08	$22,543.77	$0.00	$27,456.23
1235410180	KTRDC SHOP	Operating Expenses		$2,000.00	$1,065.92		$1,065.92		$934.08
1235410180	KTRDC SHOP	Recharges			$7.74		$7.74		($7.74)
1235410180	Result	Total		$2,000.00	$1,073.66		$1,073.66		$926.34
1235410240	KTRDC LABORATORY EQUIPMENT	Operating Expenses		$40,000.00	$14,790.79	$1,848.85	$16,639.64		$23,360.36
1235410240	Result	Total		$40,000.00	$14,790.79	$1,848.85	$16,639.64		$23,360.36
1235410250	KTRDC UNALLOCATED RESERVE FOR RESEARCH	Operating Expenses		$90,000.00					$90,000.00
1235410250	Result	Total		$90,000.00					$90,000.00
1235410280	KTRDC GENERAL LABORATORY	Operating Expenses		$50,000.00	$11,266.21	$1,137.76	$12,403.97	$0.00	$37,596.03
1235410280	KTRDC GENERAL LABORATORY	Recharges			$984.02	$1.45	$985.47		($985.47)
1235410280	Result	Total		$50,000.00	$12,250.23	$1,139.21	$13,389.44	$0.00	$36,610.56

FISCAL YEAR 2025-2026 INCOME AND FINANCIAL REPORT KTRDC 3rd QUARTER REPORT

Funds Center	Funds Center Name	Category	Original Budget	Annual Budget	Prior Month Balance	Current Month Actual	YTD Actual	YTD Encumbrances	Available Budget
1235411040	KTRDC DISCRETIONARY	Operating Expenses		$20,000.00	$3,648.59	$39.96	$3,688.55		$16,311.45
1235411040	KTRDC DISCRETIONARY	Recharges			$42.32	$0.48	$42.80		($42.80)
1235411040	Result	Total		$20,000.00	$3,690.91	$40.44	$3,731.25		$16,268.65
1235411310	KTRDC OUTREACH & COMMUNICATIONS	Operating Expenses		$20,000.00					$20,000.00
1235411310	Result	Total		$20,000.00			$0.00		$20,000.00
1235411340	GENETIC MANIPULATION OF TOBACCO TO	Salaries			$11,967.00		$11,967.00		($11,967.00)
1235411340	GENETIC MANIPULATION OF TOBACCO TO	Benefits			$683.57		$683.57		($683.57)
1235411340	GENETIC MANIPULATION OF TOBACCO TO	Operating Expenses		$30,000.00					$30,000.00
1235411340	GENETIC MANIPULATION OF TOBACCO TO	Recharges			$4,985.00		$4,985.00		($4,985.00)
1235411340	Result	Total		$30,000.00	$17,635.57		$17,635.57		$12,364.43
1235411360	PLANT BIOTECH METABOLIC	Operating Expenses		$30,000.00	$15,225.31	$2,131.69	$17,357.00	$4,669.47	$7,973.53
1235411360	PLANT BIOTECH METABOLIC	Recharges			$131.68	$55.61	$187.29		($187.29)
1235411360	Result	Total		$30,000.00	$15,356.99	$2,187.30	$17,544.29	$4,669.47	$7,786.24
1235411370	KTRDC PLANT BIOTECH - MOLECULAR	Operating Expenses		$30,000.00	$20,927.35	$967.17	$2,189.52	$0.00	$8,105.48
1235411370	KTRDC PLANT BIOTECH - MOLECULAR	Recharges			$5,121.55	$11.26	$5,132.81		($5,132.81)
1235411370	Result	Total		$30,000.00	$26,048.90	$978.43	$7,322.33	$0.00	$2,972.67
1235411380	MOLECULAR GENETICS	Operating Expenses		$30,000.00	$5,849.82	$47.75	$5,897.57	$0.00	$24,102.43
1235411380	MOLECULAR GENETICS	Recharges			$50.67	$2,174.56	$2,225.23		($2,225.23)
1235411380	Result	Total		$30,000.00	$5,900.49	$2,222.31	$8,122.80	$0.00	$21,877.20
1235411410	KTRDC GREENHOUSE	Operating Expenses		$15,000.00	$6,741.55	$1,384.41	$8,125.96		$6,874.04
1235411410	KTRDC GREENHOUSE	Recharges			$3,066.71	$65.65	$3,132.36		($3,132.36)
1235411410	Result	Total		$15,000.00	$9,808.26	$1,450.06	$11,258.32		$3,741.68
1235411570	TOBACCO MOLECULAR FARMING AGRONOMICS	Recharges			$0.00		$0.00		$0.00
1235411570	Result	Total			$0.00		$0.00		$0.00
1235412360	FLAVONOID - SMALLE	Salaries			$11,968.74	$1,619.44	$13,588.18	$4,428.20	($18,016.38)
1235412360	FLAVONOID - SMALLE	Benefits			$5,618.31	$786.37	$6,404.68	$2,153.48	($8,558.16)
1235412360	FLAVONOID - SMALLE	Operating Expenses		$30,000.00					$30,000.00
1235412360	Result	Total		$30,000.00	$17,587.05	$2,405.81	$19,992.86	$6,581.68	$3,425.46

Kentucky Tobacco
Research & Development Center